

**ARTIFICIAL GROUNDWATER RECHARGE, SAN LUIS
VALLEY, COLORADO**

by

Dan Sunada



Colorado Water

Resources Research Institute

Completion Report No. 123

**Colorado
State
University**

ARTIFICIAL GROUNDWATER RECHARGE, SAN LUIS VALLEY, COLORADO

Project No. A-050-COLO
Agreement Nos. 14-34-0001-1106
14-34-0001-2106

D. K. Sunada, J. W. Warner and D. J. Molden
Civil Engineering Department
Colorado State University

Research Project Technical Completion Report

The work upon which this report is based was supported in part by federal funds provided by the United States Department of the Interior as authorized under the Water Research and Development Act of 1978 (P.L. 95-467).

Colorado Water Resources Research Institute
Colorado State University
Fort Collins, Colorado
Norman A. Evans, Director

March, 1983

ABSTRACT

Intense use of aquifers for irrigation waters has caused groundwater storage depletion in many areas of the arid and semi-arid west, including the San Luis Valley in south central Colorado. Artificial recharge is a means of alleviating this problem. To show the practical benefits of artificial recharge to local water users, a demonstration recharge basin was operated in the San Luis Valley. Both numerical and analytical models were calibrated to the aquifer response to suggest operational policies. Analysis of the results of the demonstration project indicate that if recharge operations are conducted during the non-irrigation season when excess water is available, significant amounts of water can be added to storage and combat groundwater depletion.

One difficulty with the use of models is that the results obtained from them are hard to visualize by non-technical persons. Recently a wide variety of microcomputers have become available which are relatively inexpensive and have the capability of readily evaluating solutions which describe groundwater response to artificial recharge. Their portability and graphics features make them excellent demonstration tools. As part of this study, a computer program was written which uses Glover's (1960) solution for recharge from a rectangular basin to model artificial recharge. The program is totally interactive, extremely user friendly and runs on an Apple II+ 48K microcomputer. The model describes groundwater response to artificial recharge in an infinite, homogeneous aquifer and in a stream aquifer system and can also calculate discharge into a stream. The model is designed for use by both technical and non-technical persons and is an excellent means of transferring knowledge

from groundwater hydrologists to water users. The microcomputer model developed in this study could be used in other parts of the San Luis Valley to evaluate the benefits of artificial recharge in these other areas.

ACKNOWLEDGEMENTS

Funding for this project was from the Office of Water Resources Technology, Colorado Experiment Station Project 110 and the State Engineers Office. The project was also made possible with the support of the Trinchera Irrigation Company and the Rio Grande Water Conservancy District. The authors would like to acknowledge Robert A. Longenbaugh, former Professor of Civil Engineering at Colorado State University, now Deputy State Engineer in charge of groundwater, for initiating this study; Mr. William Cruff and the other members of the board of the Trinchera Irrigation Company for permission to use their water and for their support during the project; Mr. Ernest Chavez for his help in construction and maintenance of the recharge basin; and Mr. Fred Huss for his help in measuring the observation wells. Also the support and interest of Mr. Ralph Curtis is greatly appreciated and that of the Forbes-Trinchera Ranch and Mr. Errol Ryland for allowing us to use their property and wells.

TABLE OF CONTENTS

<u>CHAPTER</u>	<u>PAGE</u>
Abstract -----	i
Acknowledgements -----	iii
List of Figures -----	ix
List of Tables -----	xi
List of Symbols -----	xii
I. INTRODUCTION -----	1
1.1 Purpose -----	2
1.2 Scope -----	2
II. SAN LUIS VALLEY -----	4
2.1 Geology of the San Luis Valley -----	6
2.2 Hydrology of San Luis Valley -----	9
2.3 Water Use in the San Luis Valley -----	11
III. DEMONSTRATION RECHARGE PROJECT -----	12
3.1 Location -----	12
3.2 Site Geology -----	14
3.3 Project Operation -----	14
3.4 Aquifer Response to Recharge -----	16
3.5 Infiltration Rate -----	17
3.5.1 Inflow -----	17
3.5.2 Evaporation -----	18
3.5.3 Calculated Infiltration Rate -----	20
3.6 Aquifer Transmissivity and Specific Yield -----	20
IV. MODELING THE PROJECT OPERATION -----	22
4.1 Analytical Model -----	23
4.2 Numerical Model -----	24

TABLE OF CONTENTS (continued)

<u>CHAPTER</u>	<u>PAGE</u>
4.3 Calibration of the Models -----	26
4.3.1 Calibration of the Analytical Model -----	26
4.3.2 Calibration of the Finite Element Model -----	27
4.4 Simulation of Artificial Recharge -----	28
4.5 Benefits of Recharge in the San Luis Valley -----	31
4.6 Operational Suggestions -----	32
V. CONCLUSIONS -----	34
VI. REFERENCES -----	36
APPENDIX A - Comparison of Mathematical Descriptions of Artificial Recharge from Basins -----	39
A.1 General Description of Artificial Recharge from Basins -----	39
A.2 The Differential Equation Describing Groundwater Flow -----	41
A.3 Baumann's Solution for a Circular Basin -----	46
A.3.1 Baumann's Flow Function -----	47
A.3.2 Solution for Zone II -----	47
A.3.3 Solution for Zone I -----	48
A.3.4 Time Dependence of Baumann's Solution -----	49
A.3.5 Discussion of Baumann's Method -----	51
A.4 Glover's Solutions for Circular and Rectangular Basins -----	52
A.4.1 Linearizing Technique Used by Glover -----	52
A.4.2 Glover's Approach to Solving the Governing Differential Equation for Groundwater Flow -----	53
A.4.3 Instantaneous Solution for a Circular Basin -----	53
A.4.3.1 Superposition of the instantaneous solution --	55
A.4.3.2 Computer implementation of the instantaneous solution -----	55

TABLE OF CONTENTS (continued)

<u>CHAPTER</u>	<u>PAGE</u>
A.4.4 Continuous Solution -----	57
A.4.4.1 Solution at the basin center -----	58
A.4.4.2 Computer implementation of the continuous solution for a circular basin -----	59
A.4.5 Glover's Continuous Solution for a Rectangular Basin --	60
A.4.5.1 Computer implementation of Glover's solution for a rectangular basin -----	61
A.4.5.2 Superposition of Glover's solution in time ---	63
A.5 Hantush's Solution for Circular and Rectangular Basins -----	65
A.5.1 Hantush's Approach: Rearrangement of the Governing Partial Differential Equation for Groundwater Flow ----	65
A.5.2 Hantush's Linearization Technique -----	66
A.5.3 Hantush's Solution for a Circular Basin -----	66
A.5.3.1 Center basin mound height -----	67
A.5.3.2 Approximate solutions to recharge from a circular basin -----	68
A.5.3.3 Computer implementation of Hantush's solution for a circular basin -----	68
A.5.4 Hantush's Solution for a Rectangular Basin -----	70
A.5.4.1 Equivalence of Hantush's and Glover's solution for rectangular basin -----	71
A.5.4.2 Computer implementation of Hantush's solution for a rectangular basin -----	71
A.6 Rao and Sarma's Solution for a Rectangular Basin -----	72
A.6.1 Solution -----	72
A.6.2 Computer Implementation of Rao and Sarma's Solution ---	73

TABLE OF CONTENTS (continued)

<u>CHAPTER</u>	<u>PAGE</u>
A.7 Hunt's Solution for a Circular Basin -----	75
A.7.1 Hunt's Solution -----	75
A.7.2 Computer Implementation of Hunt's Solution -----	78
A.8 Finite Element Program -----	80
A.9 Comparison of Solutions -----	83
A.9.1 Determination of Integration Steps -----	84
A.9.2 Computer Time Requirements -----	86
A.9.3 Rectangular vs. Circular Basin -----	88
A.9.4 Solutions with Varying Initial Saturated Depths -----	90
A.9.5 Comparison with Field Experiment -----	93
A.10 Summary -----	93
A.10.1 Baumann's Solution -----	93
A.10.2 Glover's Solution -----	95
A.10.2.1 Circular basin solution -----	95
A.10.2.2 Rectangular basin solution -----	95
A.10.3 Hantush's Solution -----	96
A.10.3.1 Rectangular basin -----	96
A.10.3.2 Circular basin -----	96
A.10.4 Rao and Sarma's Solution -----	96
A.10.5 Hunt's Solution -----	96
A.10.6 Numerical Solution -----	97
A.10.7 Suggested Analytical Methods -----	97
Appendix B - Microcomputer Model of Artificial Recharge -----	98
B.1 Introduction -----	98
B.2 Use of Glover's Solution -----	100

TABLE OF CONTENTS (continued)

<u>CHAPTER</u>	<u>PAGE</u>
B.2.1 Use of Superposition -----	100
B.3 Program Description -----	105
B.4 Discussion -----	114

LIST OF FIGURES

<u>Figure #</u>	<u>Page</u>
1 Location of the San Luis Valley -----	5
2 View of the San Luis Valley -----	7
3 Artificial Recharge Demonstration Project Site -----	13
4 Inflow Hydrograph -----	18
5 Finite element grid of area of artificial recharge -----	25
6 Aquifer response to 5 months of artificial recharge calculated from the analytical model -----	29
7 Aquifer response to 7 months of artificial recharge calculated from the finite element model -----	29
8 Well hydrographs for 7 months of artificial recharge -----	30
9 3-months aquifer response to $T = 1000$ and $T = 10,000$ -----	32
A.1 Definition sketch of artificial recharge from basins -----	39
A.2 Volume Element -----	44
A.3 Baumann's Solution Spreading with Time -----	51
A.4 Simpson's rule and Gaussian quadrature for integrating Glover's solution -----	63
A.5 Mound profile at 30 and 60 days using Gaussian quadrature to evaluate Glover's solution for rectangular basins -----	64
A.6 Iterative technique used with Hantush's linearization -----	69
A.7 Convergence Criteria for Rao and Sarma's Solution -----	74
A.8 Hunt's Solution and Glover's Solution -----	80
A.9 Finite element grid for comparing solutions -----	82
A.10 Rectangular vs. Circular Basin -----	89
A.11 Mound rise at basin center vs. time -----	91
A.12 Mound rise at basin center vs. time -----	91
A.13 Mound profile -----	92
A.14 Mound profile -----	92

LIST OF FIGURES (continued)

<u>Figure #</u>	<u>Page</u>
A.15 Mound profile obtained from field observations and from analytical solutions -----	94
A.16 Mound rise at basin center vs. time from field observations and analytical solutions -----	94
B.1 Definition sketch of artificial recharge with a stream ----	102
B.2 Method of trapezoids to obtain discharge to the stream ----	104
B.3 Discharge to the stream vs. time -----	105
B.4 Screen Display: model options. Artificial recharge is modeled with a stream in the vicinity -----	106
B.5 Screen Display: parameter display. The depth to water is changed -----	107
B.6 Screen Display: the depth is changed from 20 to 15 feet ---	108
B.7 Screen Display: mound profile at 30 days -----	108
B.8 Screen Display: discharge to the stream at 30 days -----	109
B.9 Screen Display: output options. Create file is chosen to store data and results on the disk -----	110
B.10 Screen Display: create files. The name "Stream" is given to the input data and results calculated -----	110
B.11 Screen Display: read files. The file "No Stream" is read from the disk -----	111
B.12 Screen Display: the files "No Stream" is chosen to be plotted -----	112
B.13 Screen Display: "stream" and "no stream" will be plotted on the same graph -----	113
B.14 Screen Display: "stream" and "no stream" plotted on the same graph -----	114

LIST OF TABLES

<u>Table #</u>		<u>Page</u>
1	First 160 feet of well logs -----	15
2	Evaporation from recharge basin -----	19
3	Transmissivity obtained from specific capacity tests ----	22
4	Calculated and measured mound rise with $T = 10,000$ -----	27
A.1	Data for trial runs -----	46
A.2	Convergence of Rao and Sarma's solution -----	74
A.3	Solution obtained with differing integration steps -----	85
A.4	Computer time requirements -----	87

LIST OF SYMBOLS

- a - radius of recharge basin (L)
- A - area (L^2)
- A_i - Gaussian quadrature points
- A'_i - LaGuerre integration abscissas
- b - initial saturated thickness (L)
- B - distance to impermeable boundary (L)
- C - height of slug injected cylinder (L)
- D - radius of influence (L)
- d - denominator
- g - gravitational acceleration (L^2/T)
- h - piezometric head (L)
- H - mound height (L)
- H_o - central mound height (L)
- H_r - mound height contribution from real basin (L)
- H_{is} - mound height contribution from a basin imaged in space (L)
- H_{it} - mound height contribution from a basin imaged in time (L)
- H_{its} - mound height contribution from a basin imaged in time and space (L)
- i - integer
- j - integer
- K - hydraulic conductivity (L/T)
- L - basin length (L)

- m - integer
- M - distance to impermeable boundary (L)
- n - integer
- P - pressure (F/L^2)
- \vec{q} - Darcy velocity (L/T)
- Q - discharge (L^3/T)
- Q* - Baumann's flow function (L^3/t)
- r - radius (L)
- r_w - radius of well (L)
- R - recharge rate (L/T)
- S - storage coefficient
- S_y - apparent specific yield
- s_w - drawdown at well (L)
- t - time (T)
- T - transmissivity (L^2/T)
- u_o - $a^2/4at$
- u - variable of integration
- V - volume (L^3)
- W - basin width (L)
- W_i - Gaussian quadrature weights
- W'_i - LaGuerre integration weights
- w - volume rate of recharge (L^3/T)
- x - coordinate distance (L)
- x_i - image x coordinate (L)
- x_r - real x coordinate (L)
- y - y coordinate distance (L)

- z - vertical distance above datum (L)
- Z - $(h^2 - b^2)^{1/2}$
- α - T/S
- β - dummy variable of integration
- γ - dummy variable of integration
- ρ - density (M/L³)
- η - free surface coordinate (L)
- λ - dummy variable of integration
- τ - dummy variable of integration
- ξ - dummy variable of integration

SAN LUIS VALLEY ARTIFICIAL RECHARGE DEMONSTRATION PROJECT

CHAPTER I

INTRODUCTION

Throughout the arid and semi-arid west, productive irrigated agriculture has been made possible by extensive use of groundwater from aquifers. These aquifers are tapped year after year to supply irrigation water for the crops. In many locations more water is taken out of the aquifers and consumed by the crops than can be naturally replenished by the hydrologic cycle. Simple addition and subtraction indicates that unless the water balance of the aquifer is maintained, eventually the aquifer will become depleted.

The San Luis Valley in southern Colorado is a location where the economy and livelihood of most of the population is dependent on irrigated agriculture. In the first part of the century, groundwater was used mainly to supplement existing surface water supplies as a source of irrigation water. Today farmers rely very heavily on these underground water reserves as a major source of irrigation water. What once was thought to be an endless resource is becoming more and more precious. With the high cost of pumping and difficulties in obtaining well permits, it is clearly evident that the economic life of aquifer use is limited.

One of the best means of combating groundwater depletion is by artificial recharge. Excess surface water is pumped or allowed to percolate down to the existing groundwater. The success of artificial recharge as a management technique depends highly on how well the system is understood.

1.1 Purpose

The overall purpose of the project was to demonstrate to local water users in the San Luis Valley the feasibility of artificial recharge. Several specific objectives were met, including:

1. The successful demonstration of artificial recharge in the San Luis Valley.
2. The collection and analysis of data on the groundwater response to artificial recharge.
3. The determination of who, where and when recharge benefits occur.
4. Specific suggestions concerning artificial recharge policies consistent with the recharge facilities and water availability.
5. Evaluation of the benefits when the recharge operational policies are varied (this was performed using numerical and analytical modeling techniques).
6. Development of a method to evaluate the operation and benefits of specific recharge policies and thus to select the best operational policies for specific sites.

1.2 Scope

In order to meet the first three objectives of demonstrating artificial recharge, collecting and analyzing data and determining benefits and beneficiaries, an artificial recharge basin was constructed and operated in the winter and early spring of 1982, Employees of the Trinchera Irrigation Company and Rio Grande Water Conservancy District were directly involved in the construction and operation of the recharge basin, thus obtaining first hand experience in the practice of artificial recharge. The response of the aquifer was documented by collection of water level

measurements from nearby wells. These data on aquifer response were matched to both numerical and analytical mathematical models of artificial recharge to determine the benefits and beneficiaries of artificial recharge.

Mathematical models provide a means of suggesting operational policies and determining benefits of artificial recharge. Numerical methods, such as the finite element method, and analytical methods exist which can predict the response of the aquifer to artificial recharge. One of the problems of these mathematical models is that it is difficult to transfer the results of the complex mathematical equations to the water users. A microcomputer program was developed to transfer the knowledge by graphically displaying the response of the aquifer to artificial recharge. The model was designed for use by both groundwater specialists and non-technical water users. Specific operational policies for different sites can be developed and the benefits of artificial recharge can be visibly determined by using the program.

Analytical solutions are appropriate for this type of microcomputer program because of fast execution time and easy data input. Several analytical solutions to the artificial recharge problem have been developed yet they have not been thoroughly compared and studied to determine the applicability of each solution. Based on a review and comparison of analytical solutions, Glover's analytical solution (1960) was chosen to analyze the data obtained from the San Luis Valley and for use in the microcomputer model.

CHAPTER II

SAN LUIS VALLEY

The San Luis Valley in south-central Colorado is an arid plateau surrounded by the San Juan and Sange de Cristo mountain ranges (Fig. 1). With an abundance of water derived chiefly from snowmelt from the nearby mountain ranges, irrigation has made the valley one of Colorado's most productive agricultural regions. Although surface water supplies most of the water needs, groundwater is very heavily relied upon. Management of all water supplies is imperative for continued success of the region.

Sedimentary deposits have accumulated in the valley since the Holocene (Emery et al, 1971) epoch, creating large confined and unconfined aquifers. Since about the turn of the last century, ground water has been used extensively for agriculture, municipalities and industries. Recently the State Engineer has determined that there is little unappropriated water remaining and permits for new wells are extremely difficult to obtain.

Artificial recharge is a means of water management which could conserve this important resource. In years of high runoff, excess water could be stored in the aquifer by means of artificial recharge. Surface water which is now lost to evapotranspiration could be put into groundwater storage for future use.

A demonstration of artificial recharge was conducted in the San Luis Valley to show its beneficial use and to study the use of different mathematical models which simulate artificial recharge. Measurements

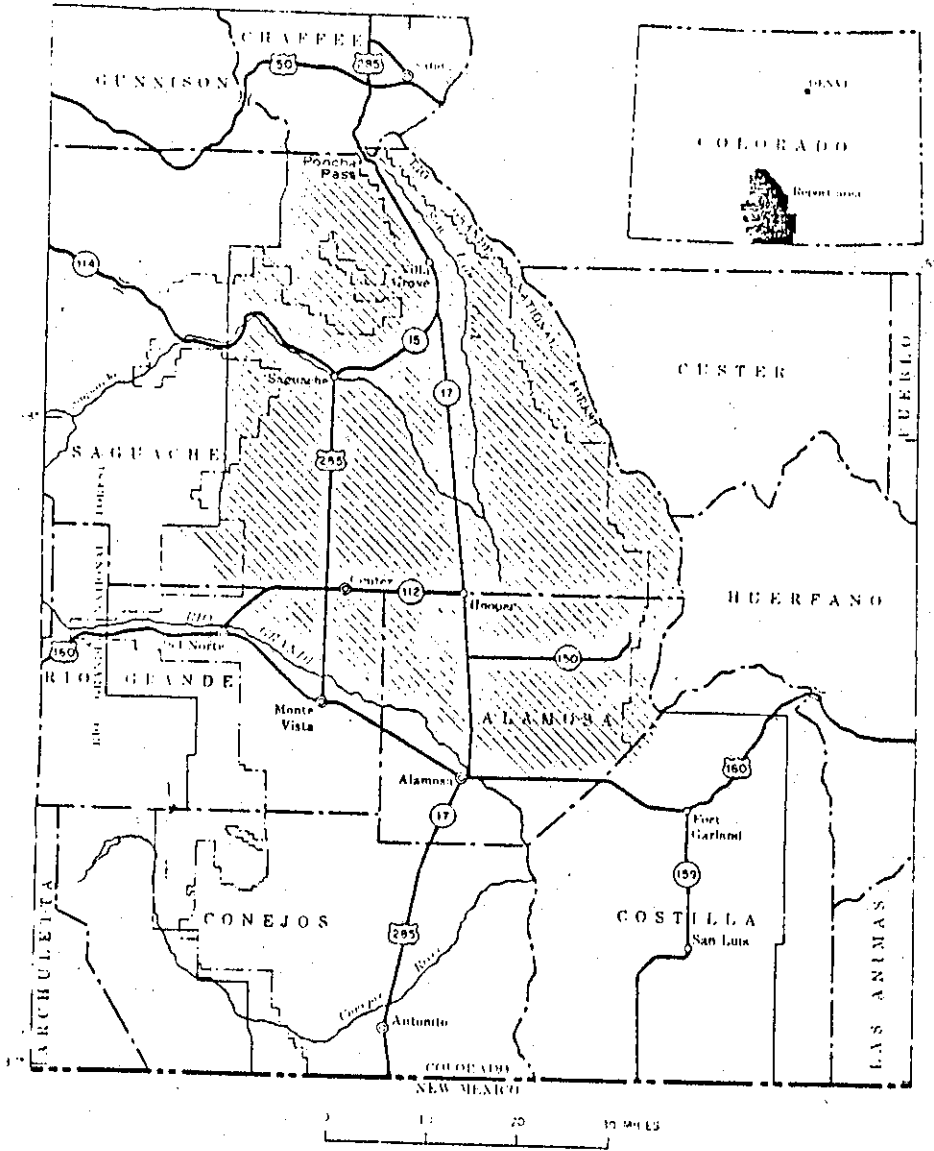


Figure 1 - Location of the San Luis Valley

(Adapted from U.S.G.S. Hydrologic Investigations Atlas HA-381)

were taken to determine infiltration and aquifer response. Both numerical and analytical models, both of which are useful management tools, were calibrated to match the aquifer response. The field project and the mathematical models demonstrate the benefits of artificial recharge as well as enable specific artificial recharge policies to be suggested.

2.1 Geology of the San Luis Valley

The San Luis Valley lies between two high mountain ranges, the San Juan mountains to the west and Sangre de Cristo mountains to the east (Fig. 2). The ranges merge at Poncha Pass to form the north boundary of the valley. From Poncha Pass the valley extends south 110 miles to about 15 miles past the New Mexico State line.

The area of the valley is about 3200 mi² with an average altitude of 7700 ft. Receiving less than 8 inches of precipitation annually, the arid high plateau experiences hot summers and cold winters with an average annual temperature of 42°F (Emery et al, 1973).

After the uplifting which formed the Sangre de Cristo and San Juan ranges, a large depression was left in between the two ranges. In the late miocene or early pleiocene epoch, alluvial fans deposited sediments characteristic of the Santa Fe formation. At the end of this period of deposition, lava flows covered much of the alluvium. During the late pleiocene or early pleistocene, a fresh water lake occupied much of the valley, leaving the lacustrine deposits characteristic of the Alamosa formation. The lake has since receded, leaving the valley in its current state. These two formations, the Santa Fe and Alamosa,

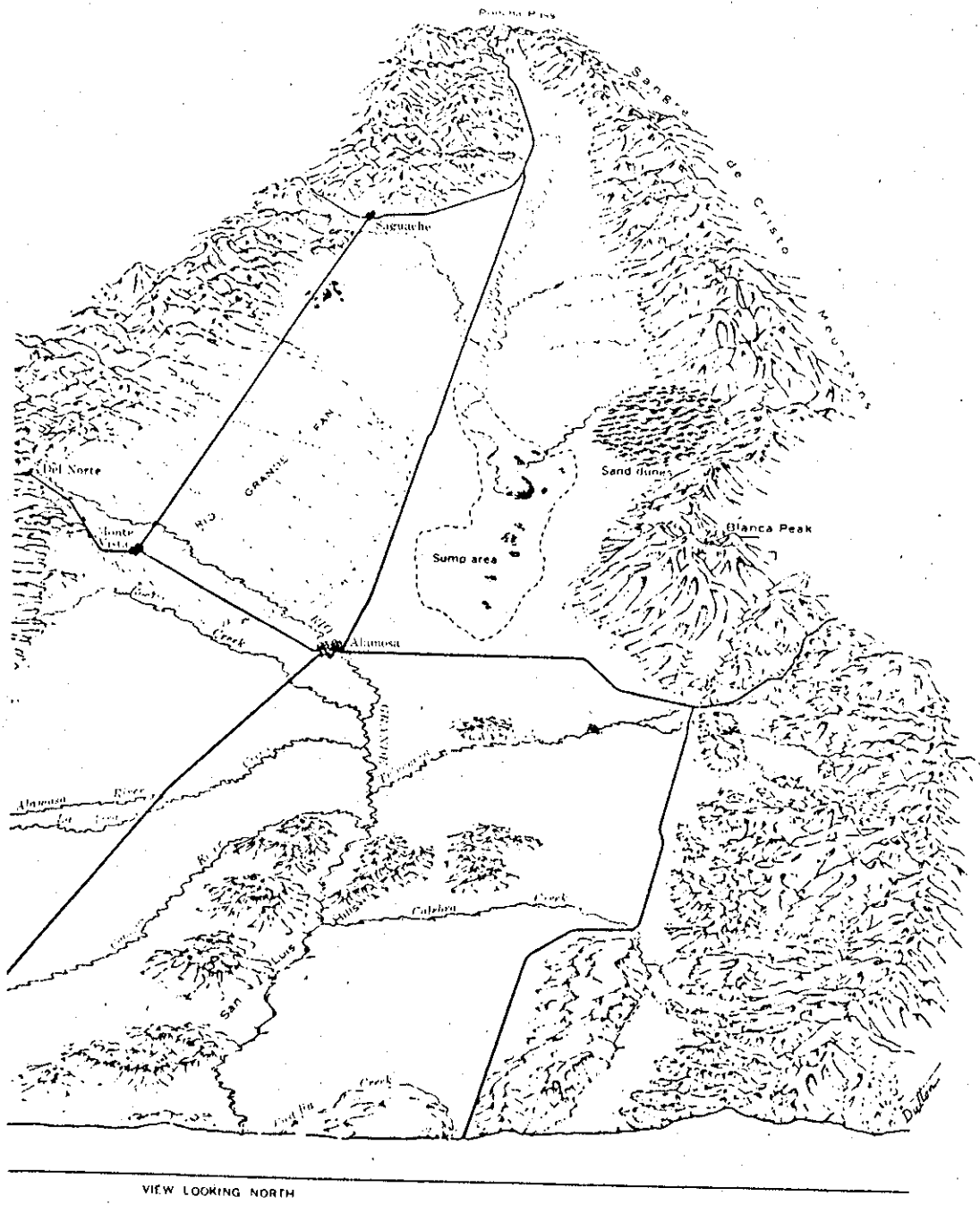


Figure 2 - View of the San Luis Valley

(Adapted from U.S.G.S. Hydrologic Investigations Atlas HA-381)

have by far the greatest hydrogeologic significance to the valley (Siebenthal, 1910).

In most of the valley, the Santa Fe formation rests on top of an impervious crystalline material and is overlain by the Alamosa formation. Emery et al (1971) reports that it is difficult to distinguish between the two formations, except locally. At the surface, the basaltic San Luis Hills stretching from Fort Garland south, are typical of the Santa Fe formation.

The Santa Fe formation is composed of clay, silt, sand, gravel and volcanic debris. The clay is described as pink, red, brown or blue and is "firm or hard and blocky". The clay layers are not of great areal extent, but are local lenticular formations. The sand is often cemented by clays or calcareous material. The well rounded shape of the sand and gravel indicates that they are alluvial deposits (Powell, 1958).

Typical of the Alamosa formation are lenses of clay interstratified with sands or unconsolidated gravel. These sediments were deposited by alluvial fans, feeding a fresh water lake. Coarser sediments are more common around the edge of the valley, whereas finer lacustrine deposits of clay and silt are more common in the center of the valley. Recent deposits overlay the Alamosa formation and are difficult to distinguish from it.

Two major aquifers, the confined and unconfined, composed of the Santa Fe and Alamosa formation are present in the valley. Confining clay or lava layers form the boundary between the two aquifers. The thickness of the formation is up to 30,000 ft. (Emery, 1972), giving the aquifers the capacity to store vast amounts of water.

2.2 Hydrology of San Luis Valley

Surface inflow is the most important source of water, averaging about 1,580,000 acre ft. per year (Emery, 1970). Precipitation contributes about 1,220,000 acre ft. per year. About 86% of this water is consumed by evapotranspiration. The remaining 14% leaves as groundwater or surface flow. Emery et al (1975) estimated there is about 2 billion acre feet of ground water in storage. With the exception of the closed basin around San Luis lake, where the water is discharged by evapotranspiration, the water is drained by the Rio Grande River.

With mountains at its perimeter and alluvium full of porous sand and gravel and confining layers of clay and lava, the valley is ideal for a very productive confined aquifer. Much of the early agricultural development of the valley was due to the existence of flowing artesian wells with heads up to 55 ft. above the land surface (Siebenthal, 1910).

Siebenthal (1910) states that "the source of supply of the artesian (confined) water in the San Luis Valley is unquestionably the mountain streams which flow down across the alluvial slopes. The disappearance of the mountain streams ... is a matter of common observation." The water is transmitted by slanting stratum where it is confined by increasingly thicker layers of clay. In addition to recharge from mountain snowmelt, recharge to the aquifer also comes from part of the Rio Grande River. Percolating irrigation water is an important source of recharge for both confined and unconfined aquifers. Precipitation, which is on the average less than 8 inches annually, is not an important source of recharge into the confined aquifer. Discharge from the confined

aquifer comes from wells, springs and upward seepage. Emery et al (1973) estimated about .6 to .8 ft. of upwards leakage per unit area into the unconfined aquifer.

At the turn of the 20th century large scale irrigation was made possible by diversion of great amounts of water by canals. Many wells tapping the confined aquifer also brought water to the surface. The percolation of this irrigation added a substantial amount of water resulting in the expansion of the unconfined aquifer. It was not until the drought of the 1930's that this unconfined aquifer was put into heavy production.

Recharge to the unconfined aquifer is mostly from irrigation water leaking from canals or percolating from fields. Other sources of recharge are from precipitation, percolation of water from flowing wells and upwards seepage from the confined aquifer. Discharge from the aquifer is from streams, evapotranspiration and from wells (Powell, 1958).

In an extensive survey, Emery et al (1972) was able to give ranges of the hydraulic properties of the aquifer in different regions of the valley. For the entire San Luis Valley area, the confined aquifer has an average storage coefficient of about 0.008 and the range of transmissivities is from 200 to 200,000 ft²/day. An average storage coefficient for the unconfined aquifer is 0.2 and the range of transmissivity is 130 to 33,000 square feet per day. For the confining layer which separates the confined and unconfined aquifers, Emery et al (1975) estimated a vertical hydraulic conductivity of .059 ft/day over most of the valley where clay is the confining layer and .00059 where lava is the confining layer. These values represent average values for the San Luis Valley and are not for the local recharge site.

2.3 Water Use in the San Luis Valley

Having an arid climate, irrigated agriculture has been important since the time the original Hispanic settlers placed the first irrigation canal in Colorado near the town of San Luis. An important historic event to the development of the valley was the discovery of a flowing artesian well in 1887 by S.P. Heine (Siebenthal, 1910). After that discovery, ground water use spread rapidly. In 1891 Carpenter (1897) estimated there were 2000 flowing wells in the valley. Siebenthal (1910) counted 3,234 flowing wells. Powell reported about 7500 flowing wells in 1946. Emery et al (1973) estimates 650 large capacity wells (>300 gpm) and about 7000 small capacity wells tapping the confined aquifer. Over 2,200 large capacity wells withdraw water from the unconfined aquifer.

In 1970 approximately 1,900 thousand acre feet of water was used in the San Luis Valley. Of this, 1,250 thousand acre feet was from surface water diversion, 400 thousand acre feet was withdrawn from the unconfined aquifer and about 250 thousand acre-feet was withdrawn from the confined aquifer (Emery, 1973). The use of water from the confined aquifer was more or less constant from 1940 to 1970, but water use from the unconfined aquifer varies inversely with stream flow.

Many water use problems have developed in the San Luis Valley. Use of surface water for irrigation has caused water logging and high consumptive use in many areas. Some soils have become alkali due to large amounts of evapotranspiration. Since 1957 deliveries of water to New Mexico and Texas have been deficient in accordance with the Rio Grande impact (Emery, 1972). Due to the lack of unappropriated water it is now very difficult to obtain permits for drilling new wells.

CHAPTER III

FIELD DEMONSTRATION RECHARGE PROJECT

3.1 Location

The recharge site is located approximately 3 miles south-east of Fort Garland in Costilla County (Fig. 1) on a Forbes-Rincheria Ranch lot. The basin is near Gaccon road, about 300 ft. west of Trincheria Canal and about 800 ft. south of the Sangre de Cristo Trincheria Division (Fig. 3).

Water obtained with permission from the Trincheria Irrigation Company was diverted from the Trincheria Canal into the basin. The water leaks from Mountain Home Reservoir into Trincheria Creek and is then diverted into the Trincheria Canal.

The project site was chosen to isolate the response of the aquifer from other aquifer stresses. Compared to other parts of the San Luis Valley, there is little irrigated agriculture nearby, so recharge of irrigation water is not a problem. Some of the large irrigation pumps in the vicinity (Fig. 3) are in use during the irrigation season but not in late fall, winter and early spring. Wells #2, 3 and 4 on Figure 3 are also available to measure aquifer response to artificial recharge. The geology is less complex in this area than other areas. The surface material is sandy and appeared to have very good infiltrating potential.

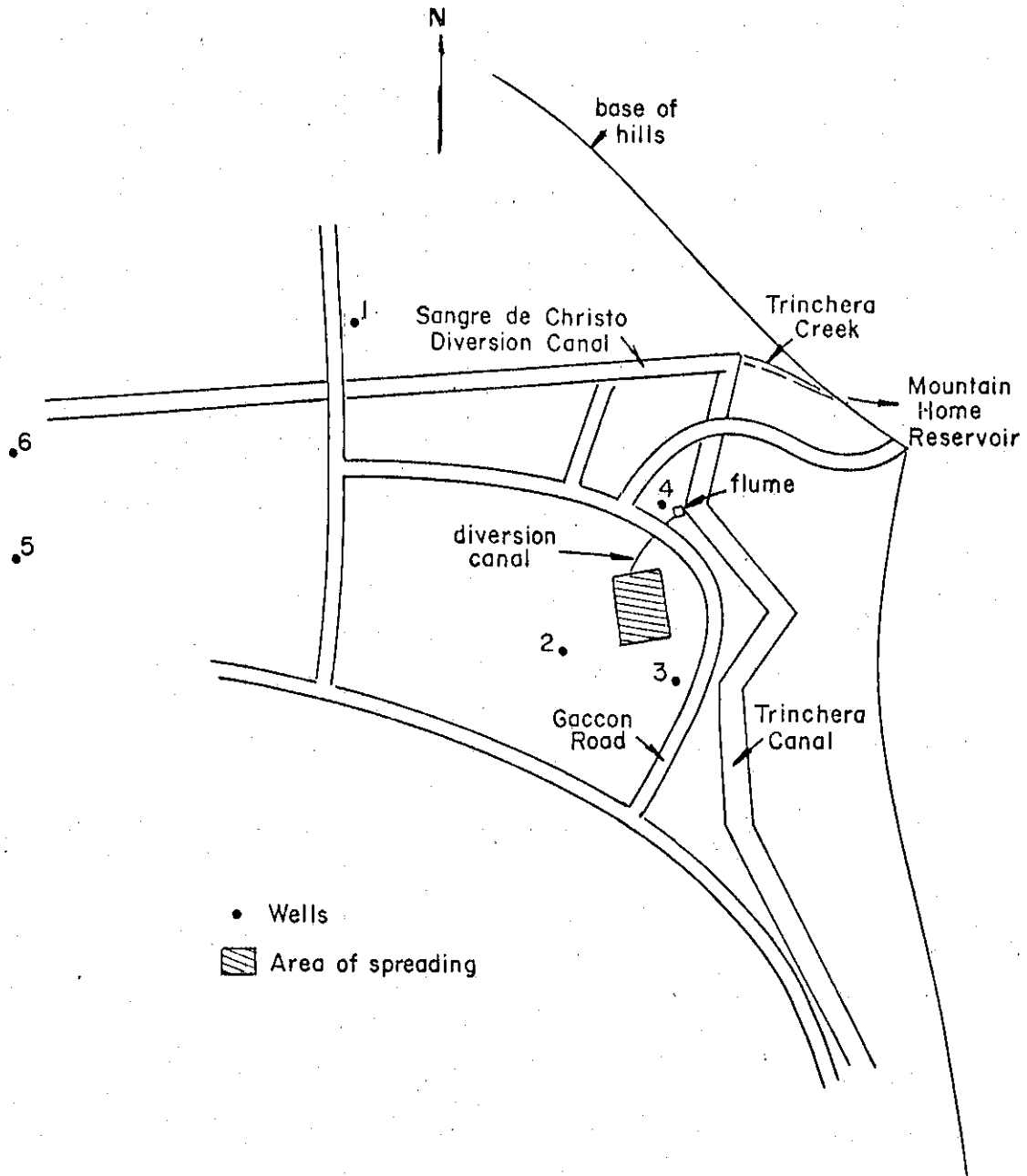


Figure 3 - Artificial Recharge Demonstration Project Site.

3.2 Site Geology

Well logs were obtained from wells 1, 3 and 4 (Table 1). These logs indicate the clay, sand and gravel typical of the Santa Fe and Alamosa formations. At the time of study the depth to water was about 100 feet. In the region above 100 feet the logs show mostly sand and gravel with some clay streaks, which should allow rapid deep percolation. There appears to be no definite confining layers in the first 180 feet from the surface. The geologic logs indicate some thick clay layers but these clay layers do not appear to be extensive and did not appear to impede the vertical movement of recharge water. Emery (1972) indicates all these wells tap the unconfined aquifer. The wells are over 500 feet deep and possibly tap both unconfined and confined aquifers.

The saturated thickness is difficult to determine as a bottom impermeable stratum cannot be distinguished on the geologic logs. It was assumed that the saturated thickness of the aquifer is about the depth of well penetration which is about 500 feet.

3.3 Project Operation

The recharge basin was excavated in late fall 1981, to a size of about 200 feet by 140 feet. The depth of the recharge basin was about 1 to 2 feet. The excavated top soil was used as retaining dikes of about 1 to 3 feet in height surrounding the recharge basin. An inlet channel was constructed to convey water from the Trinchera canal to the recharge basin (Figure 3). Near the site of diversion a cutthroat

TABLE 1. First 160 feet of well logs

Depth (ft)	Well 1	Well 3	Well 4
10	sand and gravel	sand and clay	sand and gravel
20			
30	brown clay		sand and gravel
40	brown clay and sand		gravel and clay
50			
60	sand and gravel		
70			gravel and clay
80	gravel		
90			
100			
110	sand and clay	small gravel and sand	gravel and clay streaks
120			
130			
140	brown clay and sand		
150			
		small gravel and sand	hard gravel

flume was installed to measure inflow. Inflow into the Trinchera canal was controlled by a gate at Trinchera Creek, which allowed adjustment of the size of the pond in the recharge basin. The start of the operation was delayed until early spring.

The recharge operation started February 24, 1982 and water was recharged for a period of 49 days. A total volume of about 1,123,000 cubic feet of water was recharged during the operation. Periodic well measurements were taken during and after the recharge period to measure the response of the aquifer. On April 14, 1982, well number 1 began pumping for irrigation water and the project came to a close.

At the beginning of the operation, a large amount of sediment was carried into the basin. The silting of the basin caused a reduction of the infiltration rate, so the level of water in the basin had to be checked frequently. Daily operation of the recharge basin was handled by personnel of the Trinchera Irrigation District, allowing the local personnel in the San Luis Valley to gain experience in artificial recharge.

3.4 Aquifer Response to Recharge

Well elevations and recharge basin elevations were obtained by survey. In this report, all elevations were taken with respect to a local reference point.

Wells 2, 3 and 4 (Figure 3) were used as observation wells to measure the response of the aquifer. Measurements started in March 1982 and continued throughout the entire project. The initial conditions were those measurements taken the day of startup. After 41 days well 2 showed a rise of .43 ft., well 3 a rise of .62 ft. and well 4 a rise

of .61 ft. Well measurements were made by personnel of the Rio Grande Conservancy District.

3.5 Infiltration Rate

To obtain the infiltration rate a mass balance given by: inflow + precipitation-evaporation = infiltration, was performed. This mass balance assumes steady state conditions where the depth of the pond stays constant. This steady state approximation is good except during small times such as the turn on and shut off of inflow water.

3.5.1 Inflow

Inflow was measured by a cutthroat flume placed near the site of diversion. The flume was 5 feet in length with a 4 inch throat. The flow depth, measured immediately before the throat, was measured by a float in the stilling basin. A Steven's type F water stage recorder was used with a 32 day clock to record the depth of flow.

The flow rating was determined by the relationship (Skogerboe et al, 1973).

$$Q = 1.265 h_a^{1.69} \quad (1)$$

where

$$Q = \text{discharge (cfs)}$$

and

$$h_a = \text{flow depth (ft).}$$

From the chart paper, flow depths were averaged over eight hour periods. The inflow hydrograph is given on Figure 4. The total volume of inflow was 1,151,000 cubic feet of water. Precipitation during the recharge period was small, resulting in a total volume of 1160 cubic

feet of water. Any daily precipitation recorded in the nearby town of Blanca was added to the inflow.

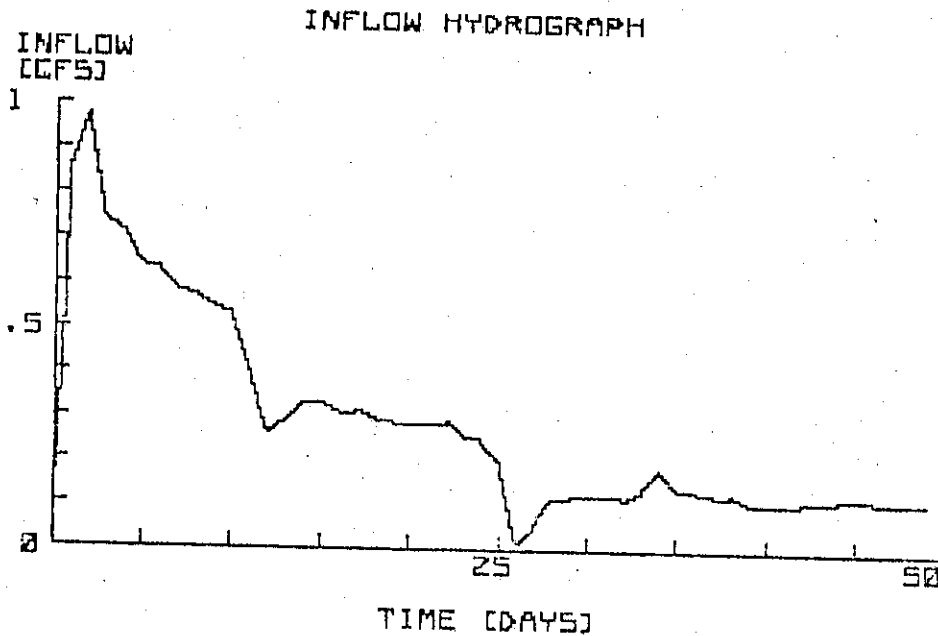


Figure 4 - Inflow Hydrograph

3.5.2 Evaporation

To estimate evaporation, a nomograph from Linsley, Kohler and Paulhus (1975) was used. Mean daily temperature, dewpoint temperature, wind velocity and net solar radiation are the necessary parameters to calculate evaporation.

The nomograph relies heavily on mean daily temperature which was accurately measured. Mean daily temperatures were obtained from the nearby town of Blanca. The mean dewpoint temperature was estimated to be 0°C. Net radiation was estimated at 700 Langley's which is

slightly greater than the clear day solar radiation for the period of recharge. It was observed that there was a great deal of wind during the project operation, so a wind speed of 140 miles per day was used (which is an extremely large value for average daily wind speed).

The calculated values for evaporation are given in Table 2.

TABLE 2 - Evaporation From Recharge Basin

Period	Average Temperature °F	Evaporation (in/day)	Evaporation (ft/day)
2/24 - 2/28	33.3	0.22	0.018
3/1 - 3/15	32.5	0.22	0.018
3/16 - 3/31	35.0	0.23	0.019
4/1 - 4/14	40.0	0.27	0.022

Assumptions

Dew Point Temp. = 0°F

Wind Velocity = 140 mi/day

Solar Radiation = 700 Lanley's/day

An evaporation pan was operated during the second half of April. This allowed a comparison between evaporation estimated from the nomograph to that measured by the evaporation pan. The pan evaporation for the second half of April was 3.83 inches or an average rate of .225 inches per day. The calculated evaporation using all the assumptions for

dewpoint, solar radiation and wind movement was 6.40 inches or an average rate of .376 inches per day.

The total calculated evaporation from the recharge basin was 48,720 cubic feet, which is only 2.5 percent of the inflow. The calculated evaporation using the nomograph most likely overestimated the actual evaporation but because evaporation was very small compared to inflow, any errors introduced were negligible.

3.5.3 Calculated infiltration rate

The infiltration rate in feet per day was calculated by dividing the net infiltration volume by the area over which the water was spread. The average infiltration rate over the recharge period was about 1.04 ft. per day. During the first 25 days of recharge, the water was maintained in a 200' x 100' area and the average recharge rate was 1.82 ft. per day. For the last 24 days, when water spread outside of the basin due to collapse of the dike, the average infiltration rate was .22 feet per day. The low infiltration rate for the last 24 days reflects a doubling of area over which water was spread.

3.6 Aquifer Transmissivity and Specific Yield

Emery (1972) conducted specific capacity tests in the region and reported a range of transmissivities between 3000 and 17,000 ft²/day around the area of the recharge site. Data was available from the geologic logs of wells near the recharge site to estimate transmissivity by the specific capacity method.

Neglecting well losses, the equation for specific capacity using the logarithmic approximation for the well function is (Todd, 1980)

$$\frac{Q}{s_w} = \frac{4\pi T}{(2.30) \ln(2.25 Tt/r_w^2 S)} \quad (2)$$

where

s_w = drawdown at the well

and

r_w = radius of the well.

Following the work of Emery, the storage coefficient in equation (2) was set at 0.2.

The geologic logs for wells 1, 2, 4, 5 and 6 had specific capacity information to obtain transmissivity of the aquifer by equation (2). In all cases, the drawdown, discharge and radius of the well were given. The logs did not contain the duration of the specific capacity tests. The time was guessed to be 24 hours. Time does not affect the calculation of transmissivity by equation (2) much, because time is contained in the logarithmic term. Erroneous discharge and drawdown have a much greater effect on the calculated transmissivity. Table 2 summarizes the results of transmissivities for these wells.

To study the sensitivity of the method, a storage coefficient of .1 changes the value of transmissivity near well 5 and 6 from 5760 to 6130 ft²/day. A storage of .2 but a time of 1/2 day changes the transmissivity to 5380 ft²/day. From these specific capacity tests it can be concluded that the transmissivity is on the order of 7500 ft²/day. Perhaps the best estimate of transmissivity was obtained from calibrating the artificial recharge models to the actual field data.

TABLE 3 - Transmissivity obtained from specific capacity tests.

Well	Q (cfs)	(ft)	r _w (in)	T (Ft ² /day)
1	3.00	34	10	7550
1*	1.41	32.6	8	3380
2	3.68	30	10	10940
4	6.6	59**	10	9330
5	2.7	38	9	5760
6	2.7	38	9	5760

*records of a pump test supplied by Trinchera Ranch.

**estimated drawdown.

CHAPTER IV

MODELING THE PROJECT OPERATION

By accounting for the movement of artificially recharged water, mathematical models aid in determining the operational policies and benefits of artificial recharge. The models have the advantage that they can transfer the results of the demonstration artificial recharge to other sets of hydrologic and operational conditions. For example, the models can be used to predict aquifer response to varying recharge rates, varying recharge times or changes in aquifer characteristics. The field problem also provides a practical example of the application of mathematical models to predict mound geometry. Warner's finite element flow model (1981) and Glover's solution for a rectangular basin (1960) were both used.

The analytical model (Glover's) was used in calibration because it is fast and easy to use. The numerical model (Warner's) was used in calibrations because a boundary was present and the operation did not have a constant recharge rate and basin size over time. These conditions are too hydrologically complex for the simplifying assumptions of Glover. After the models were calibrated, they were perturbed to suggest operational policies.

4.1 Analytical Model

To use the analytical model, several simplifying assumptions were made. The aquifer was assumed to be homogeneous, isotropic, infinite in areal extent with an initial horizontal water table. In actuality,

the aquifer has layers of interbedded sand, gravel and clay and is not homogeneous in a vertical cross section (Table 1). Areal, the aquifer is composed of sand and gravel with some clay streaks with no apparent large inhomogeneities. No data are available to take into account areal inhomogeneities and the use of constant areal transmissivity in the model is thought to be valid. The aquifer has a large saturated depth at the project site, so the linearizing assumption of constant transmissivity in time is thought to be valid.

There is no flow boundary which at its closest point is about 1500 feet away from the recharge site. The boundary is far enough away that it should not affect the shape of the recharge mound.

The slope of the water table at the recharge site was very small and an initial horizontal water table was used in both analytical and numerical models.

4.2 Numerical Model

The grid system (Figure 5) used by the finite element model was constructed to include the no-flow boundary. The location of the no-flow boundary is approximately at the base of the hills (Figure 3). The remaining boundaries are no-flow but are placed at large enough distances away from the project site that they will not greatly affect flow due to recharge.

The assumptions of homogeneous, isotropic aquifer with an initially horizontal water table were also used in the finite element model. During calibration, the variable recharge rate and area of spreading were taken into account.

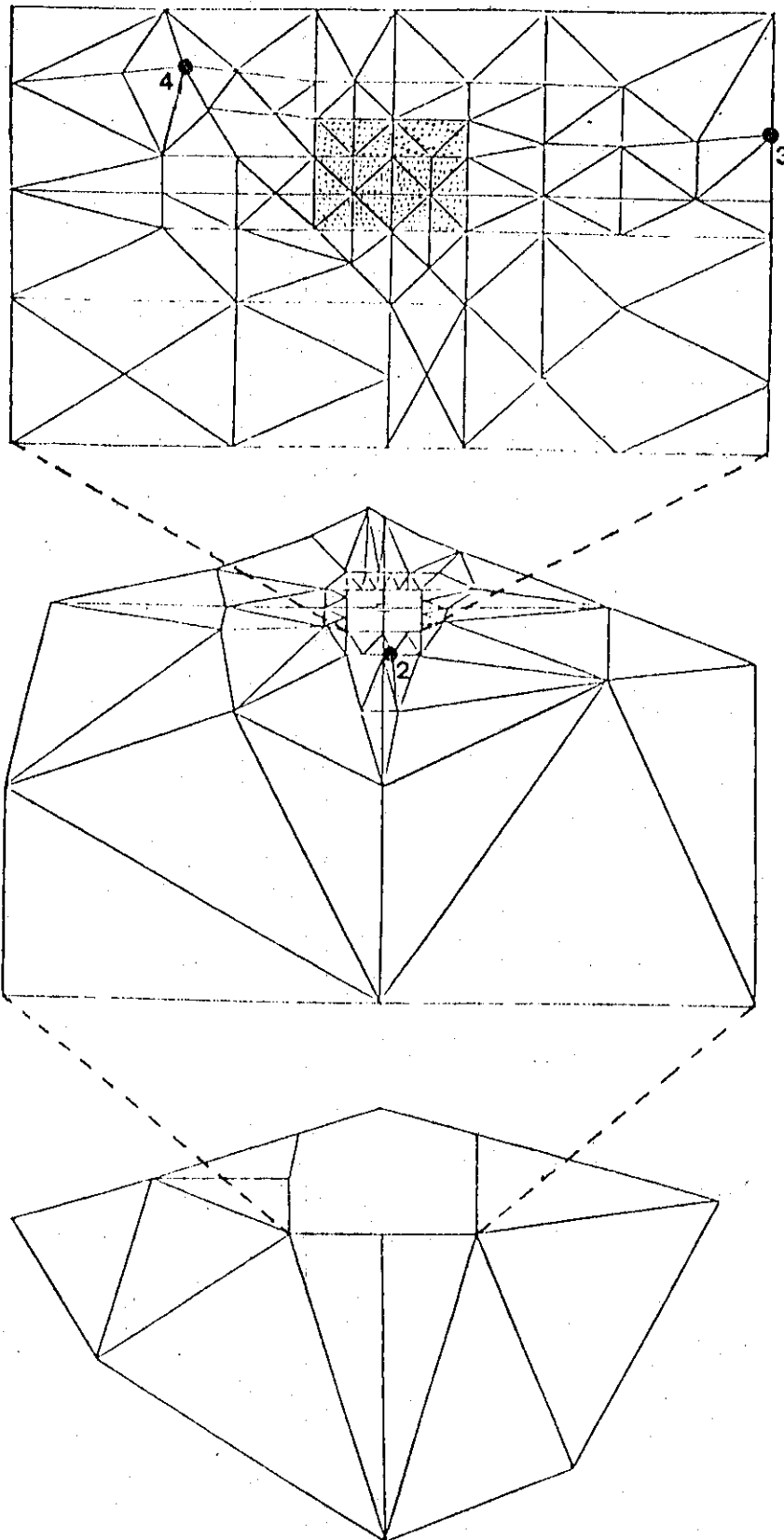


Figure 5 - Finite element grid of area of artificial recharge. Shaded area represents basin.

4.3 Calibration of the Models

To calibrate the models, the aquifer response calculated by the model was compared with the aquifer response measured in the field. In both models, the storage coefficient was set at 0.2. Only large deviations in the storage coefficient will greatly affect results obtained by the model. Transmissivity was varied until the model calculations gave a best fit to the measured field values. The lag time between the first day of infiltration and the first day of aquifer response was taken into account on all calibration runs.

4.3.1 Calibration of the analytical model

Using the analytical solution, transmissivities between 10,000 and 15,000 ft²/day simulate the field results fairly well. A constant recharge rate of 1.82 ft/day was used for the entire recharge period and the change in the recharge area was not taken into account. The recharge area was set at 180' by 200' covering the western portion of the basin (Figure 3). The calculated and actual field data are shown in Table 4.

TABLE 4 - Calculated and Measured Mound Rise with $T = 10,000$.

Time (days)	Well No.	Measured Height (ft)	Calculated Analytical (ft)	Height Numerical (ft)
22	4	0.49	0.57	0.56
22	3	0.45	0.39	0.35
22	2	0.20	0.33	0.30
41	4	0.61	0.95	0.71
41	3	0.62	0.72	0.63
41	2	0.43	0.72	0.55

4.3.2 Calibration of the finite element model

The finite element model took into account the change in recharge rate and change in area of the basin. For the first 25 days the recharge rate was set at 1.82 ft/day spreading over a 100' by 200' area. For the next 24 days the recharge rate was set at 0.22 ft/day spreading over an area twice as large, the extra 100' by 200' area spreading towards well 2 (Figures 3 and 4). The calculated and measured mound heights compare very well. Using a transmissivity of $10,000 \text{ ft}^2/\text{day}$, the maximum difference between observed and calculated response was about 0.12 ft. As a calibration parameter $10,000 \text{ ft}^2/\text{day}$ agrees well with the specific capacity tests and was the homogeneous transmissivity used in the simulation runs.

4.4 Simulation of Artificial Recharge

The calibrated models were used to predict the aquifer response to a different sequence of recharge events. One of the best policies would be to operate the recharge basin as much as possible when the water is not needed for irrigation. During the coldest winter months it is assumed that recharge would not be possible because the water would freeze. The hypothetical recharge operation considered on the model was to recharge from October to December, shut the operation down in January to February, then begin recharging again in March and April. The periods of recharge are highly weather dependent so the cycle would never be exactly like this. However, this hypothetical example will allow the benefits of a sustained recharge operation to be studied.

The entire existing 200' by 140' basin was used with a constant recharge rate of 1.8 feet per day. From the actual recharge operation, this appears to be the maximum rate the soil will allow over a long time period. The water table was assumed to be initially horizontal and the natural and artificial (i.e. pumping) water table fluctuations were neglected. The obtained results may be superimposed on these fluctuations. Figure 6 gives the results using Glover's solution for the first five months.

The results obtained by the finite element solution for the recharge operation from October to March are shown in Figure 7. These values were obtained along the center line of the basin parallel to the length (200 ft) axis. The results are slightly higher than those obtained with

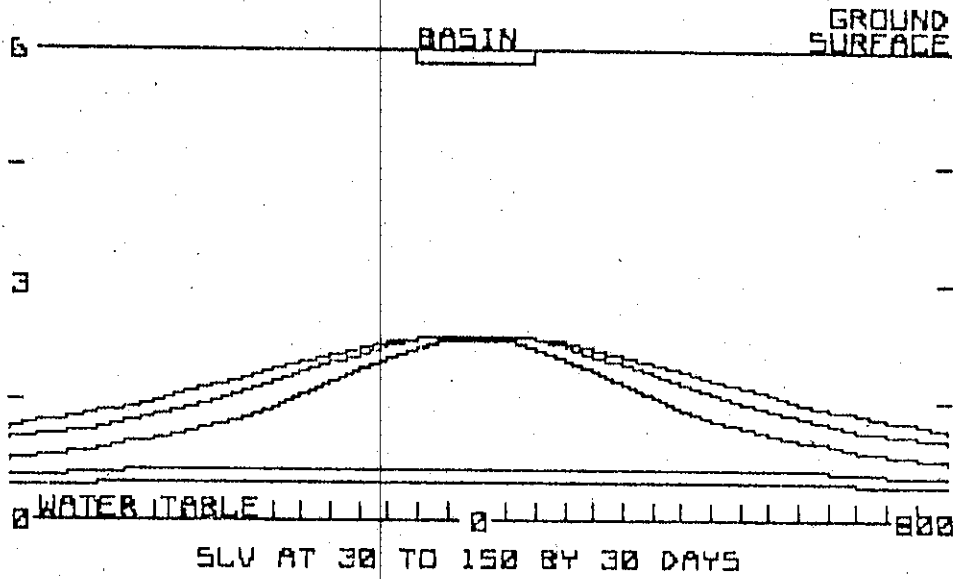


Figure 6 - Aquifer response to 5 months of artificial recharge calculated from the analytical model.

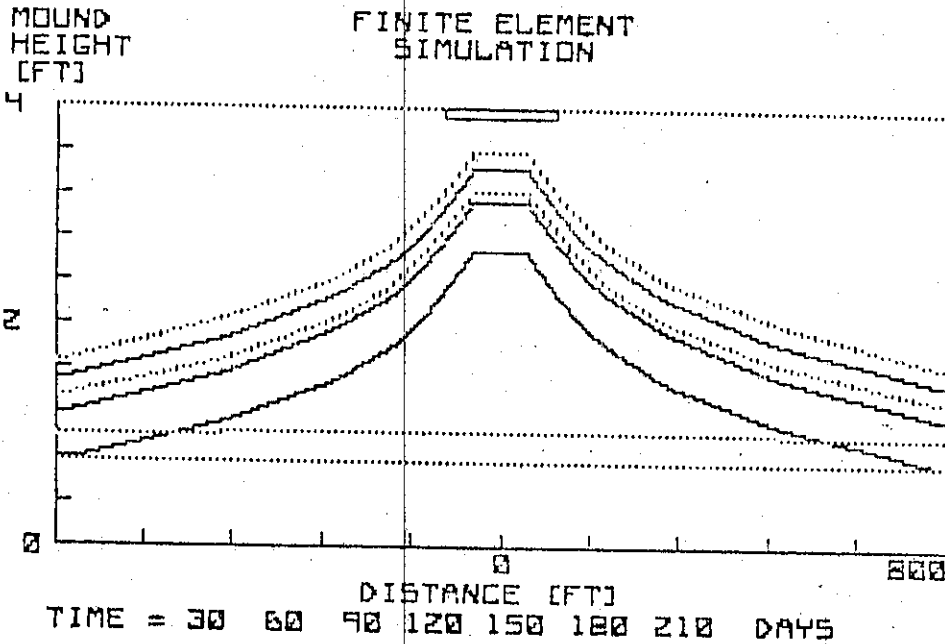


Figure 7 - Aquifer response to 7 months of artificial recharge calculated from the finite element model. The first 3 months are the solid line, the next 4 months are the dotted line.

the analytical solution probably due to the presence of the impermeable boundary.

Hydrographs of wells 2, 3 and 4 calculated from the finite element model are shown in Figure 8. The water levels in each of the wells rose approximately 2 feet.

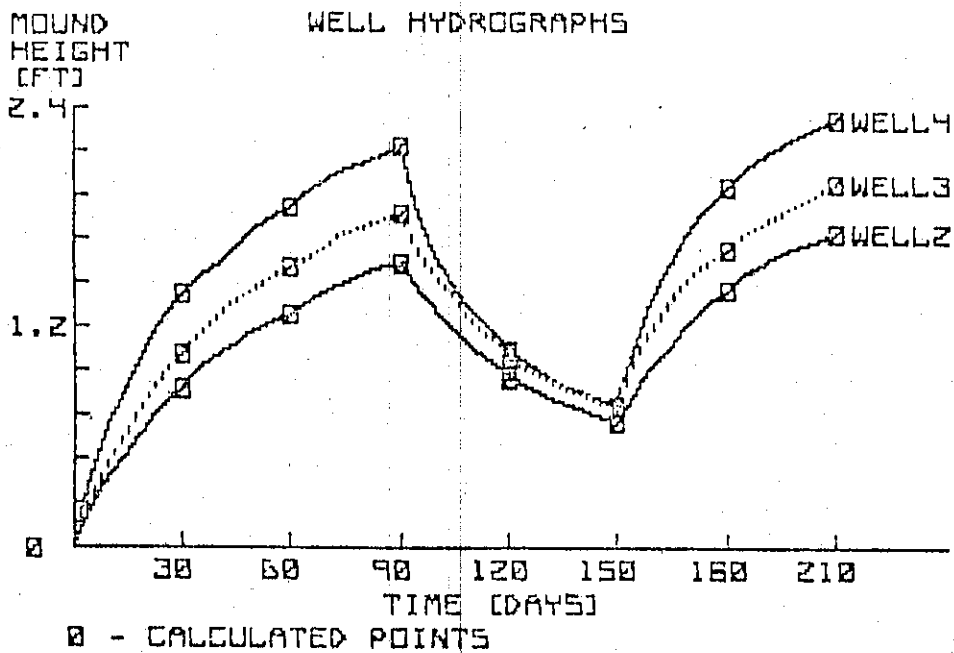


Figure 8 - Well hydrographs for 7 months of artificial recharge.

Another simulation run was made with the analytical model with a constant recharge rate of 1.82 feet per day assuming a sustained seven months recharge operation. The rise at the center was about 3.5 feet which was not significantly greater than the center mound height shown in Figure 6. Due to high transmissivities the water table does not rise

a great deal in response to recharge. However, the water does spread rapidly to enhance aquifer storage at large distance from the recharge basin.

4.5 Benefits of Recharge in the San Luis Valley

A tangible benefit of artificial recharge is the reduced cost of pumping due to raising water table. For a radius of more than 1000 feet around the recharge basin the water was raised approximately two feet. In this case, the high transmissivity is ideal because all the large capacity wells (wells 1 to 6, Figure 3) near the recharge basin would benefit from the raised water table.

If the same recharge operation were performed in another location where the transmissivities are lower the mound build up near the basin would be much greater. Figure 9 shows the mound buildup when the transmissivity is $1000 \text{ ft}^2/\text{day}$ compared to the simulation run where the transmissivity was $10,000 \text{ ft}^2/\text{day}$. In an area of low transmissivity, placing a recharge basin near an existing well would greatly reduce pumping lift.

Raising the water table 2 feet a year is substantial over a long time period. This long range benefit of artificial recharge is less tangible than reducing pumping lifts but is more important. Heavy dependence on the aquifer will eventually cause serious aquifer depletion. Over the long run, the benefits of a resource cannot be continually enjoyed unless they are replenished. Adding one or two feet of water to the aquifer may not seem significant but if excess surface waters are efficiently recharge at many sites, this yearly addition to the aquifer can become very significant.

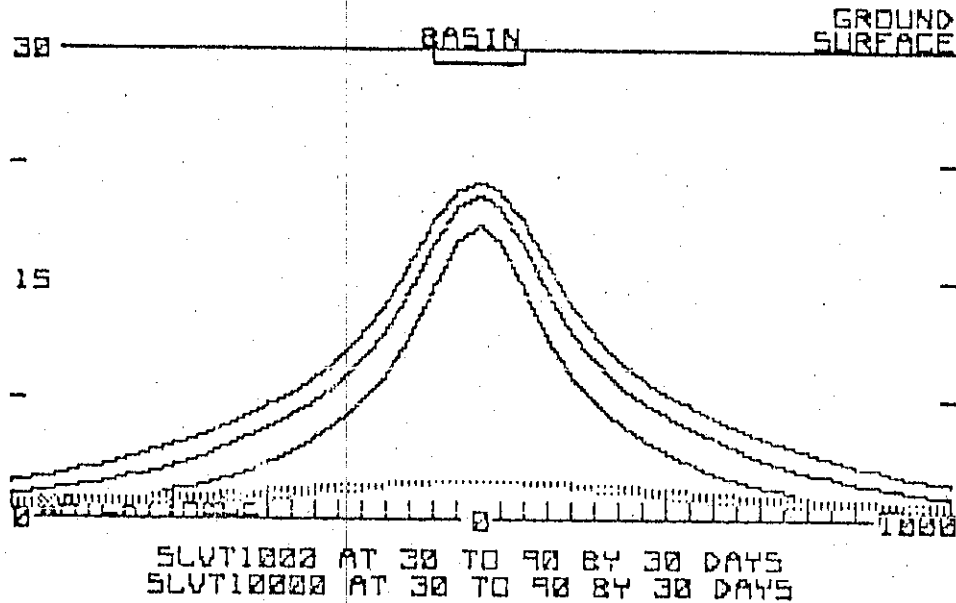


Figure 9 - 3-months aquifer response to $T = 1000$ (solid line) and $T = 10,000$ (dotted line).

4.6 Operational Suggestions

A successful recharge operation demands more than spreading water over a permeable surface. Continual maintenance and support by local water users is necessary to obtain all the potential benefits of artificial recharge. From the experience of this demonstration project some operational policies are suggested.

Incoming sediments greatly reduce the recharge rate. In the San Luis Valley there are two significant sources of sediment, the inflowing water and the wind. To prevent sediments from inflowing water to spread over the entire basin, the depth of the basin should be dug deeper near the entrance to the basin. This deeper area will cause most sediments to settle in one isolated area. There is not much that can be economically done to retard incoming sediments carried by the wind.

Over time, the bottom of the basin will become silted, reducing the recharge rate. The water level in the pond must be continually checked and the inflow rate adjusted when necessary, to prevent overflowing. During periods when the recharge basin is not in use, the bottom should be scraped and roughened to increase the potential recharge rate.

The basin should be made as level as possible. If it is not level, water should enter at the high point of the basin to ensure that the basin gets filled. The basin should be dug to a depth of about two or three feet. The retaining dikes should not be heavily relied upon to hold the water so the depth of water should not be allowed to rise far above the surrounding ground surface.

CHAPTER V

CONCLUSIONS

An artificial recharge basin was successfully operated in spring of 1982. The recharge basin construction, operation and maintenance was done in cooperation with the Trinchera Irrigation Company giving them first hand experience in artificial recharge.

Data was collected prior to, during and after the recharge operation. All the wells within a 600 foot radius from the basin showed a half foot rise in water level due to artificial recharge.

Numerical and analytical modeling calibrated on the aquifer response were used to predict aquifer response to a different set of conditions. The models showed that mound build up was not large due to high transmissivity. The recharging water spread rapidly increasing storage in a large area surrounding the basin.

The models were used to vary operational policies consistent with recharge facilities and water availability. The models showed that if water is recharged during the non-irrigation season excepting those months when water would freeze, one foot of water would be added to aquifer storage for a radius of at least 1000 feet from the recharge basin. This one foot may not seem significant but if the practice is continued year after year, aquifer depletion will be retarded and more water will be in storage for drought years.

Artificial recharge benefits all water users in the area surrounding the recharge basin by adding water to storage. The long term benefits of artificial recharge will be the greatest because of retardation of

aquifer depletion. Water recharged during years of high surface runoff is kept in storage for drought years.

A microcomputer model was developed (Appendices A and B) as a means of evaluating the operation and benefits of specific recharge policies. The microcomputer model can be used to display aquifer response to local water users.

REFERENCES

- Abramowitz, M. and I. A. Stegun, 1972. Handbook of mathematical functions with formulas, graphs and mathematical tables. 8th ed., Dover Publications, Inc., New York, N.Y., 1046 pp.
- Baumann, P., 1952. Groundwater movement controlled through spreading. Transactions, ASCE, v. 117, pp. 1024-1060.
- Bear, J., 1979. Hydraulics of Groundwater. McGraw-Hill, Inc., 567 pp.
- Bianchi, W.C. and E.E. Haskell, 1966. Air in the vadose zone as it affects water movement beneath a spreading basin. Transactions, ASAE, vol. 15, pp. 103-106.
- Bianchi, W.C. and E.E. Haskell, 1968. Field observations compared with the Dupuit-Forchheimer theory for mound heights under a recharge basin. Water Resources Research, vol. 4, no. 5, pp. 1049-1057.
- Bianchi, W.C. and E.E. Haskell, 1975. Field observations of transient groundwater movement produced by artificial recharge into an unconfined aquifer. Agricultural Research Service W-27, 27 pp.
- Bittinger, M.W. and F.J. Trelease, 1965. The development and dissipation of a ground-water mound. Transactions, ASAE, v. 8, pp. 103-104, 106.
- Butalla, M.W., 1982. Microcomputers: Do they have a place in large engineering firms? Civil Engineering, ASCE, v. 52, no. 6, June.
- Campbell, H.E. and P.F. Dierker, 1978. Calculus with analytical geometry. Prindle, Weber and Schmidt, Inc., Boston, Mass. 878 pp.
- Carpenter, L.G., 1891. Artesian wells of Colorado and their relation to irrigation. Colorado Agricultural College Experiment Station Bulletin 16., pp. 17-27.
- Dallaire, G., 1982. The microcomputer explosion in CE firms. Civil Engineering, ASCE, v. 52, no. 2, pp. 45-50. February.
- Dvoracek, M.J. and S.H. Peterson, 1971. Artificial recharge in water resources management. Journal of Irrigation and Drainage, Div. ASCE, v. 97, no. IR2, pp. 219-232.

- Emery, P.A., 1970. Electric analog model evaluation of a water-salvage plan, San Luis Valley, South Central Colorado. Colorado Ground Water Circular No. 14, 11 pp.
- Emery, P.A., A.J. Boettcher, R.J. Snipes and H.J. McIntyre, Jr., 1971. Hydrology of the San Luis Valley, South-Central Colorado. U.S.G.S. Hydrologic Investigation, Atlas HA-381.
- Emery, P.A., R.J. Snipes, J.M. Dumeyer, 1972. Hydrologic data for the San Luis Valley, Colorado. Colorado Water Resources Basic-Data Release No. 22, 146 pp.
- Emery, P.A., R.J. Snipes, J.M. Dumeyer and J.M. Klein, 1973. Water in the San Luis Valley, South-Central Colorado. Colorado Water Resources Circular No. 29, 21 pp.
- Freeze, R.A., 1971. Three dimensional, transient, saturated-unsaturated flow in a ground water basin. Water Resources Research, v. 14, pp. 844-856.
- Glover, R.E., 1960. Mathematical derivations as pertain to groundwater recharge. Agricultural Research Service, USDA, Ft. Collins, Colo.
- Hantush, M.S., 1967. Growth and decay of groundwater-mounds in response to uniform percolation. Water Resources Research, v. 3, pp. 227-234.
- Hunt, B.W., 1971. Vertical recharge of unconfined aquifers. Journal of Hydraulic Div., ASCE, v. 97, no. HY7, pp. 1017-1030.
- Kashkuli, H.A., 1981. A numerical linked model for the prediction of the decline of groundwater mounds developed under recharge. Ph.D. Dissertation, Colorado State University, Ft. Collins, CO, 142 pp.
- Linsley, R.K., M.A. Kohler and L.H. Paulhus, 1975. Hydrology for Engineers. McGraw Hill, Inc., p. 167.
- Marino, M.A., 1974. Water table fluctuations in response to recharge. Journal of Irrigation and Drainage Division, ASCE, vol. 100, no. IR2, pp. 117-125.
- McWhorter, D. and D.K. Sunada, 1977. Ground water hydrology and hydraulics. Water Resources Publications, Ft. Collins, Colorado, 290 pp.
- Ortiz, N.V., 1977. Artificial groundwater recharge with capillarity, Ph.D. dissertation, Colorado State University, Ft. Collins, CO., 88 pp.
- Pinder, G.F. and W.G. Gray, 1977. Finite element simulation in surface and subsurface hydrology. Academic Press, N.Y., 295 pp.
- Powell, W.J., and P.B. Mutz, 1958. Ground-water resources of the San Luis Valley, Colorado. U.S.G.S. Water Supply Paper 1379, 284 pp.

Prickett, T.A., 1979. Ground-water computer models - state of the art. Ground Water, v. 17, lp. 167-173.

Rao, N.H. and P.B. S. Sarma, 1981. Ground-water recharge from rectangular areas. Ground Water, Vol. 19, no. 3, pp. 270-274.

Siebenthal, C.E., 1910. Geology and water resources of the San Luis Valley, Colorado. U.S.G.S. Water Supply Paper 240, 128 pp.

Skogerboe, G.V., R.S. Bennett and W.R. Walker, 1973. Selection and installation of cutthroat flumes for measuring irrigation and drainage water. Colorado State University Experiment Station, Ft. Collins, Technical Bulletin 120, pp. 4-7.

Todd, D.K., 1980. Groundwater Hydrology. John Wiley & Sons, New York, N.Y., 535 pp.

Warner, J.W., Finite Element 2-D transport model of groundwater restoration for in situ solution mining of uranium. Ph.D. dissertation, Colorado State University, Ft. Collins, CO, 320 pp.

APPENDIX A
 COMPARISON OF MATHEMATICAL DESCRIPTIONS OF ARTIFICIAL RECHARGE
 FROM BASINS

A.1 General Description of Artificial Recharge from Basins

Although there are many means of artificial recharge, only recharge from two-dimensional basins is described here. To operate the basin, water is spread over a large surface area and allowed to infiltrate. The water percolates downward until it is refracted by the water table, resulting in the growth and spreading of a recharge mound (Fig. A.1).

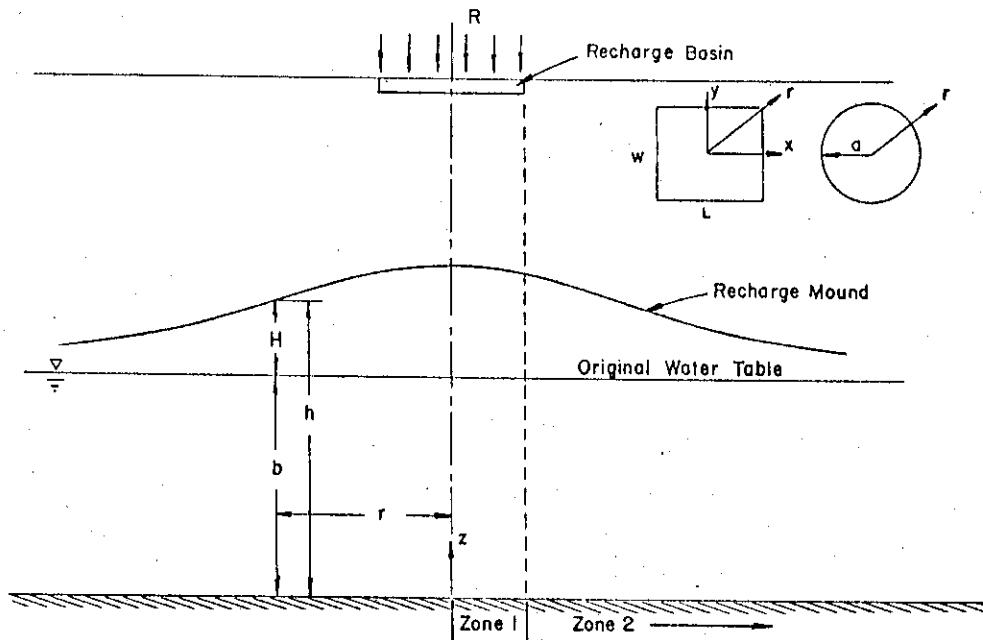


Figure A.1 Definition sketch of artificial recharge from basins.

The vertical movement of percolating water depends on the initial water content of the geologic profile, the vertical hydraulic conductivity of the geologic medium and air entrapped beneath the wetting front. Only movement of water in the saturated zone will be mathematically described, but it is important to understand how the movement through the unsaturated zone affects the validity of the saturated models. In field situations it is difficult to determine the time of travel from the ground surface to the water table. Water may pass through different geologic stratum with varying hydraulic properties which might impede vertical flow and cause spreading. Air beneath the advancing wetting front moves laterally, causing a rounded shape of the wetting front (Bianchi and Haskell, 1966). Even though the recharge rate at the surface may be constant in time, it may take some time after the wetting front reaches the water table before a constant recharge rate is obtained. For descriptions of artificial recharge which include the unsaturated zone see Freeze (1971), Kashkuli (1981) and Ortiz (1977).

The shape of the mound depends upon the recharge rate, the size of the basin and the hydraulic characteristics of the soil. A greater ease of lateral movement (transmissivity) will allow water to spread rapidly, thus impeding the vertical growth of the mound. If the porosity and storage capabilities of the soil are high, the vertical growth and spreading of the mound will be slowed down.

The shape of the mound is important for many reasons. The increased height of the water table at the location of a well will decrease pumping lifts. Seasonal fluctuations of the water table influenced by artificial recharge can be studied. If a stream is in the vicinity, it may be important to know how much recharging water is discharged into

the stream. To avoid drainage problems, the water table should not come too close to the land surface. For these reasons the design of a basin and recharge rate are influenced by the mound geometry.

Solutions have been developed to describe artificial recharge. These solutions use different boundary conditions, basin shapes and linearization techniques. First the derivation of partial differential equations used to formulate the solutions is outlined.

A.2 The Differential Equation Describing Groundwater Flow

There are many approaches to solve the problem of the recharge mound geometry. These approaches use different linearizing assumptions and different boundary conditions. To test the validity and show the limitations of the solutions for artificial recharge mound geometry, the assumptions and equations used must be clearly stated. Although the derivation of partial differential equations for groundwater flow are well documented (for example: McWhorter and Sunada, 1977, Todd, 1980; Bear, 1979) it is useful to outline these derivations and state the assumptions used.

Analytical solutions for artificial recharge consider an unconfined aquifer in which the pressure of the free surface is atmospheric. The first two assumptions made are that the aquifer is isotropic and has an impermeable bottom.

The Dupuit Forchheimer assumptions offer a means to express discharge in an unconfined aquifer. These assumptions state that if the slope of the water table is small, the pressure head distribution in a cross section is hydrostatic and the flow is horizontal in a cross section (McWhorter, Sunada, 1977). This allows flow in two dimensions to be considered.

The Darcy velocity is given by

$$\vec{q} = - K \nabla h \quad (A.1)$$

where

$$\vec{q} = \text{Darcy velocity (L/T)}$$

$$K = \text{hydraulic conductivity (L/T)}$$

$$h = \frac{P}{\rho g} + z, \text{ the piezometric head (L)}$$

$$P = \text{pressure (M/T)}$$

$$\rho = \text{density of water (M/L}^3\text{)}$$

$$g = \text{gravitational acceleration (L}^2\text{/T}^2\text{)}$$

$$z = \text{elevation above a datum (L)}$$

and

$$K = K(x, y)$$

$$h = h(x, y)$$

$$\nabla = \left(\frac{\partial}{\partial x} \vec{i} + \frac{\partial}{\partial y} \vec{j} \right)$$

The flow per unit width of aquifer, Q , is then given by

$$Q = - K \nabla h. \quad (A.2)$$

In an unconfined aquifer there are three storage mechanisms: water compression, aquifer expansion and filling of the pores. Filling of pore spaces is far more important than the other two mechanisms for increasing the volume of an aquifer. Apparent specific yield, S_y , is used to describe the storage properties of an unconfined aquifer, where S_y is defined as the volume of water released per unit area per unit decline in head, or

$$S_y = \frac{\Delta V}{A \Delta h} \quad (A.3)$$

where

$$V = \text{volume (L}^3\text{)}$$

$$A = \text{area (L}^2\text{)}$$

$$\begin{aligned} & \left[\left(Q_x \Big|_{x=\delta x} - Q_x \Big|_{x=0} \right) + \left(Q_y \Big|_{y=\delta x} - Q_y \Big|_{y=0} \right) - W \right] \delta t \\ & = \left[\left(\frac{\partial}{\partial x} Q_x \Big|_{x=0} \right) \delta y + \left(\frac{\partial}{\partial y} Q_y \Big|_{y=0} \right) \delta x - w \right] \delta t \end{aligned} \quad (\text{A.6})$$

From the definition of specific yield, the volume change in storage is

$$S(\delta x \delta y) \delta h = S_y(\delta x \delta y) [h(t+\delta t) - h(t)] \quad (\text{A.7})$$

The continuity equation now can be written as

$$\left[\left(\frac{\partial}{\partial x} Q_x \Big|_{x=0} \right) \delta x + \left(\frac{\partial}{\partial y} Q_y \Big|_{y=0} \right) \delta y + w \right] = S_y(\delta x \delta y) [h(t+\delta t) - h(t)] \quad (\text{A.8})$$

Specific yield, S_y , is replaced by an equivalent term, S , the storage coefficient. Using Darcy's law to substitute for Q_x and Q_y , dividing both sides by $\delta x \delta y \delta t$, and letting $\delta x, \delta y, \delta t \rightarrow 0$, the equation becomes

$$\frac{\partial}{\partial x} \left(K h \frac{\partial h}{\partial x} \right) + \frac{\partial}{\partial y} \left(K h \frac{\partial h}{\partial y} \right) + \dot{w}/\Lambda = S \frac{\partial h}{\partial t} \quad (\text{A.9})$$

which is the non-linear equation for a non-homogeneous isotropic aquifer. Numerical methods, such as finite difference and finite element methods can be used to solve this equation.

If the aquifer is homogeneous ($K = \text{constant}$), the equation is written

$$\frac{\partial}{\partial x} \left(h \frac{\partial h}{\partial x} \right) + \frac{\partial}{\partial y} \left(h \frac{\partial h}{\partial y} \right) + \frac{R}{K} = \frac{S}{K} \frac{\partial h}{\partial t} \quad (\text{A.10})$$

where

$$R = \text{recharge rate } (L^3/T \cdot L^2)$$

The derivation of the partial differential equations will follow a volume balance approach assuming that the compressibility of water can be neglected (Bear, 1979). Consider a volume element with horizontal area $\delta x \delta y$ (Fig.A.2). The volume balance can be stated as the volume inflow minus the volume outflow is equal to the negative of the time rate of change of storage within the element. In the case of recharge, the vertical accretion is an important source of inflow.

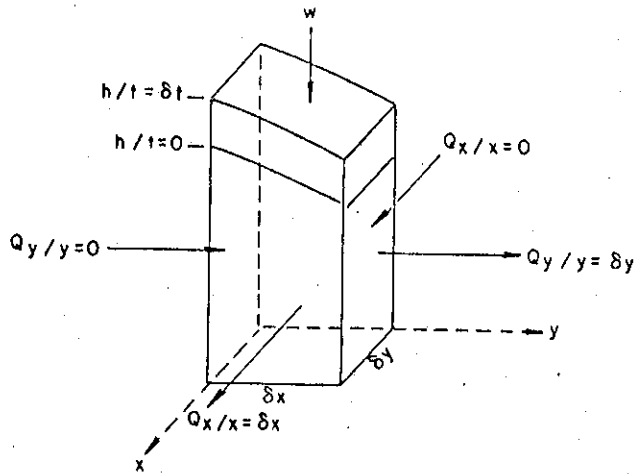


Figure A.2. - Volume Element

Using a Taylor's series expansion neglecting higher order terms.

$$Q_x \Big|_{x=\delta x} = Q_x \Big|_{x=0} + \left(\frac{\partial}{\partial x} Q_x \Big|_{x=0} \right) \delta x \quad (\text{A.4})$$

$$Q_y \Big|_{y=\delta y} = Q_y \Big|_{y=0} + \left(\frac{\partial}{\partial y} Q_y \Big|_{y=0} \right) \delta y \quad (\text{A.5})$$

Outflow minus inflow during time δt becomes

which is the non-linear Boussinesq equation. Because of the non-linearity the equation is difficult to solve by analytical methods, so linearizing assumptions are made.

To linearize the equation, an average saturated depth, \bar{b} , needs to be defined. Using this constant, \bar{b} , and the definition of transmissivity,

$$T = K \bar{b}' \quad (\text{A.11})$$

where

$$T = \text{transmissivity } (L^2/T)$$

equation (2.10) can be written as

$$T \left(\frac{\partial^2 h}{\partial x^2} + \frac{\partial^2 h}{\partial y^2} \right) + R = S \frac{\partial h}{\partial t} \quad (\text{A.12})$$

This form of the differential equation for groundwater flow is used to obtain all the analytical solutions except Baumann's.

It is important to know which equation to use for a given field problem. A comparison of each solution was made to give suggestions on their use. Each solution is stated. Because computers are needed in analyses of these equations, the numerical methods used to evaluate each solution is described. To compare solutions, numerical values were given to each parameter to test the sensitivity of each solution to the parameters (Table A.1).

TABLE A.1 Data for Trial Runs

Recharge Rate	=	1.0 ft/day
Hydraulic Conductivity	=	10.0 ft ² /day
Initial Saturated Depth	=	20, 50, 200, 100 ft
Storage Coefficient	=	.20
Time	=	stated in examples
Basin Width	=	200 ft.
Basin Length	=	200 ft
Equivalent Radius	=	112.8 ft

A.3 Baumann's Solution for a Circular Basin

To obtain a solution, Baumann (1952) assumes the mound develops from a constant volume rate of recharge, w , from a circular basin of radius a . To describe the mound two zones are defined: zone I, which is the horizontal area from the center of the basin extending to the radius, and zone II, which extends from the edge of the basin to a distance D , where the mound height, H , is zero (Fig. A.1). The mound growth is transient with distance D changing with time.

Baumann is unique in that he does not start with the governing partial differential equation but uses another strategy for obtaining separate solutions for zones I and II. He first defines a flow function Q^* which can be used to describe flow in zones I and II.

A.3.1 Baumann's Flow Function

The flow function which Baumann defines meets four conditions to describe the flow of groundwater due to artificial recharge. The first condition is that the volume rate of flow leaving zone I is equal to the volume rate of flow entering zone II. The next three conditions describe the flow as it reaches the radius of influence, D . The radius of influence acts like an impermeable boundary across which no flow crosses. At the radius of influence there is no slope to the water table. The flow approaches zero as it approaches the radius of influence. These conditions are expressed mathematically as

$$1) Q^* = w \text{ at } r = a \quad (A.13)$$

$$2) Q^* = 0 \text{ at } r = D \quad (A.14)$$

$$3) dH/dr = 0 \text{ at } r = D \quad (A.15)$$

$$4) Q^* \longrightarrow 0 \text{ at } r = D \quad (A.16)$$

Baumann's flow function which meets these conditions has an exponential form

$$Q^* = w \left[1 - \frac{\exp(r)}{D} \left(\frac{r-a}{D-a} \right) \exp(-r/L) \right]. \quad (A.17)$$

A.3.2 Solution for Zone II

The flow function, Q^* , is equated to the flow obtained by Darcy's law to obtain a differential equation for zone II.

$$Q^* = - 2\pi r(H+b) K \frac{dH}{dr} \quad (A.18)$$

for

$$a \leq r \leq D.$$

The solution of this differential equation yields the mound height for any distance r in zone II.

$$H = -b + \left(b^2 - \frac{R}{\pi K} \left\{ \ln \frac{a}{D} - \frac{1}{D-a} \left[(r+D-a) \exp \frac{D-r}{D} - 2D+r \right] \right\} \right)^{\frac{1}{2}} \quad (\text{A.19})$$

A.3.3 Solution for Zone I

Underneath zone I, Baumann assumes that the volume rate of flow of recharging water entering a circular area of radius r , is equal to the volume rate of flow leaving the same circular area of radius r . The volume rate of flow leaving the circular area of radius a can also be found by Darcy's law. The differential equation describing this volume flux is written

$$2\pi r^2 = \frac{W r^2}{a^2} = 2\pi r (H+b) K \frac{dH}{dr} \quad (\text{A.20})$$

for

$$0 \leq r \leq a.$$

Solution of the differential equation yields the expression for mound height in zone I.

$$H = -b + \left[(H_0 + b)^2 - \frac{W r^2}{2\pi K a^2} \right]^{\frac{1}{2}} \quad (\text{A.21})$$

where

$$H_0 = \text{mound height at } r = 0.$$

The central mound height is still unknown but can be found by equating the expression for mound heights in zone I and zone II at the edge of the recharge basin ($r = a$). Algebraic rearrangement gives the solution for center mound height from equations (A.20) and (A.21).

$$H_0 = -b + \left(b^2 - \frac{W}{\pi K} \left\{ \ln \left(\frac{a}{D} \right) \left[\frac{D \exp \left(\frac{D-a}{D} \right) - 2D+a}{D-a} \right] - \frac{1}{2} \right\} \right)^{\frac{1}{2}} \quad (\text{A.22})$$

A.3.4 Time Dependence of Baumann's Solution

Nowhere in the solutions for mound height does any reference to time appear and Baumann gives no clear means of finding the distance to the radius of influence. The solution is commonly mistaken to represent a steady state solution. He does give an expression for volume underneath the recharge mound which was used to relate the distance to the radius of influence to a time, t .

The volume of water stored by the recharge mound is equal to the volume rate of recharge multiplied by time.

$$V = wt = \frac{S_w}{Kb} \left\{ \frac{D^2}{4} + \frac{8D^3 - \frac{5}{2}D^2a - Da^2 + \frac{1}{2}a^3}{D-a} \right. \quad (\text{A.23})$$

$$\left. - \frac{\exp[(D-a)/D]}{D-a} (3D^3 + 2D^2a) + \frac{1}{2}a^2 [\ln(a/D) - \frac{1}{2}] \right\}$$

Dividing through by the volume rate of recharge, w , gives an expression for the time at which a given radius of influence is reached. The equation is still not in a useful form. A means of obtaining the radius of influence corresponding to a given time is needed.

Equation (A.23) is highly non-linear in D and a solution relating D to t cannot be found, so a trial and error technique was used in this study. Newton's method (Campbell and Dierker, 1979) is used to solve for D given t , because it is easy to implement on a computer and leads to quick convergence. The general form of Newton's method is

$$D_{n+1} = D_n - \frac{f(D)}{f'(D)} \quad (\text{A.24})$$

where n is the iteration step. Using equation (A.23) to obtain $f(D)$, differentiating $f(D)$ and substituting these into equation (A.24) gives

$$\begin{aligned}
D_{n+1} = D - \left\{ \frac{S}{Kb} \left[\frac{D^2}{4} + \frac{8D^3 - \frac{5}{2}D^2a - Da^2 + \frac{1}{2}a^3}{(D-a)} - \frac{\exp\left(\frac{D-a}{D}\right)(3D^3 + 2D^2a)}{D-a} \right. \right. \\
\left. \left. + \frac{a^2}{2} \left(\ln\left(\frac{a}{D}\right) - \frac{1}{2} \right) \right] - t \right\} \div \\
\left(\frac{S}{Kb} \left[\frac{D}{2} + \frac{16D^3 - 26.5D^2a + 5Da^2 + \frac{1}{2}a^3}{(D-a)^2} \right. \right. \\
\left. \left. - \frac{\exp\left(\frac{D-a}{D}\right)}{(D-a)^2} (6D^3 - 4aD^2 - 5a^2D - 2a^2) - \frac{a^2}{2D} \right] \right) .
\end{aligned} \tag{A.25}$$

A first guess of D as well as the given time, t_i , must be supplied to the right hand side of the equation to calculate D_{n+1} . D_{n+1} is then substituted for D in the right hand side of the equation. The process is repeated until the calculated D_{n+1} matches D . As a suggestion, an initial guess of $D = 10a$ causes fast convergence.

The entire mound profile at any time can now be found. D is first found for the specified time by equation (A.25). The central mound height H_0 is next found by equation (A.22). H_0 is substituted into equation (A.21) to find the solution for mound height in zone I. Equation (A.19) gives the mound height in zone II. Example mound profiles are given in Fig. A.3 with the data given in Table A.1 with $b = 50$ ft. The plot was done on an Apple II computer with points calculated on the Cyber 720 from the appropriate equations.

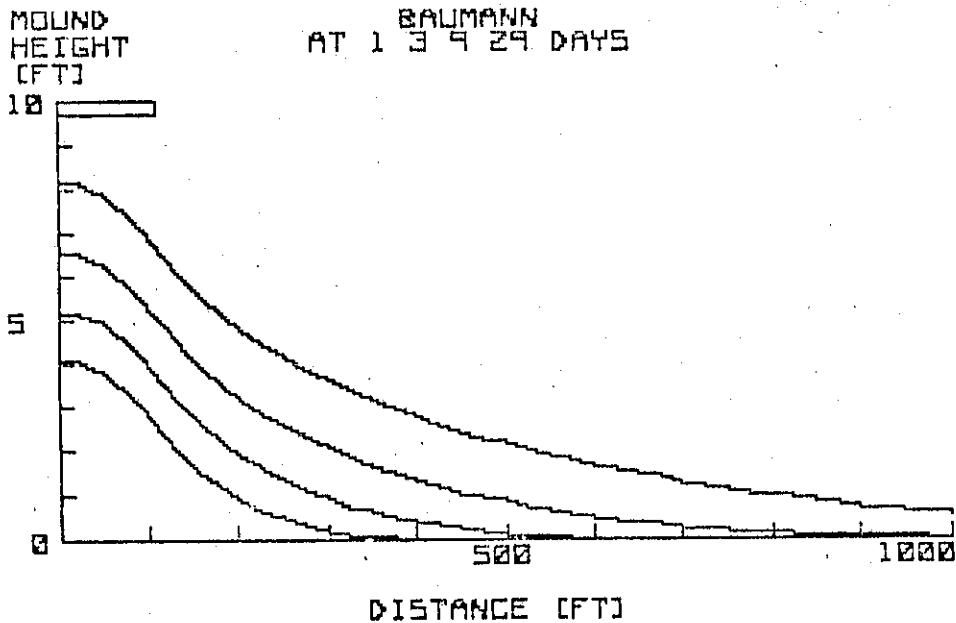


Figure A.3 - Baumann's Solution Spreading with Time.

A.3.5 Discussion of Baumann's Method

The validity of Baumann's method may be questioned because his solutions are not obtained from the governing partial differential equations. The conditions he uses to describe flow under zone I are not accurate. Condition 1 (equation A.13 and equation A.20) states that the volume entering an area of radius, r , equal the volume leaving this same area. This implies there is no change in storage under zone I. Certainly, the buildup of the mound underneath the recharge basin is due to water kept in storage.

Baumann uses a radius of influence which acts as an impermeable boundary and spreads in time. This assumption, that the recharge mound spreads with time, may be more appropriate than assuming that there is an instantaneous response over the entire aquifer.

The flow function that Baumann defines may seem arbitrary but was found to do a good job in describing the groundwater response to artificial recharge. The equations that Baumann uses are all algebraic requiring no summations. The iterative procedure to find D must be performed once per time step. Baumann's solution thus has the advantage of being easy to program.

A.4 Glover's Solutions for Circular and Rectangular Basins

Glover (1960) was the first to obtain solutions for artificial recharge using the governing differential equations for groundwater flow. He presents an instantaneous solution for the case of recharge from a circular basin, and a continuous solution for the case of a rectangular basin. Glover's instantaneous solution for a circular basin was extended to the more useful case of continuous recharge.

A.4.1 Linearizing Technique Used by Glover

Glover assumes that the initial saturated thickness, b , represents an average saturated thickness at any time during the aquifer response to recharge. This approximation is good if the actual saturated thickness, h , at any given time is approximately equal to b , or that the mound rise, H , is small compared to b . The transmissivity stays constant in time and space and is written

$$T(x,y,t) = Kb \quad (A.26)$$

This technique is widely used and has led to many important solutions to groundwater problems.

A.4.2 Glover's Approach to Solving the Governing Differential

Equation for Groundwater Flow

To obtain solutions for artificial recharge, Glover superimposes line sources, injecting water into the initial saturated thickness of the aquifer over the area of the recharge basin. The volume of water injected is equal to the volume of water recharged. With this technique of introducing sources, the vertical accretion is equal to 0. Glover's solution is in terms of mound height, H , so equation (A.12) must be rearranged. Let

$$h = H + b \quad (\text{A.27})$$

and

$$\alpha = T/S. \quad (\text{A.28})$$

Substituting these into equation (A.12), accounting for R in the boundary conditions, the differential equation

$$\frac{\partial^2 H}{\partial x^2} + \frac{\partial^2 H}{\partial y^2} = \frac{1}{\alpha} \frac{\partial H}{\partial t} \quad (\text{A.29})$$

is obtained. Glover does not start from this point to obtain solutions, rather he presents solutions which satisfy this equation.

A.4.3 Instantaneous Solution for a Circular Basin

The linearized Brussinesq equation in radial coordinates analogous to equation (A.29) is (Glover, (1960)

$$\alpha \left(\frac{\partial^2 H}{\partial r^2} + \frac{1}{r} \frac{\partial H}{\partial r} \right) = \frac{\partial H}{\partial t} \quad (\text{A.30})$$

By superimposing line sinks to simulate a slug injection of a cylinder of water of height C , Glover presents a solution describing the mound spreading due to an instantaneous injection of water. The initial conditions are

$$H(r,0) = C \quad 0 \leq r \leq a \quad (\text{A.31})$$

$$H(r,0) = 0 \quad r > a. \quad (\text{A.32})$$

where C is the height of the cylinder of water equal to the volume of the water recharged divided by the area of the basin divided by the storage coefficient. This can be viewed as placing a cylinder of water with cross sectional area equal to the recharge basin area, over the aquifer and releasing it at time zero.

The boundary condition is that at an infinite distance from the basin center there is no mound rise, or

$$H(\infty, t) = 0 \quad (\text{A.33})$$

A solution satisfying the differential equation (A.30) and initial and boundary conditions is

$$H = C \left(\frac{1}{2\alpha t} \right) \int_0^a \xi \exp - \left(\frac{r^2 + \xi^2}{4\alpha t} \right) I_0 \left(\frac{r\xi}{2\alpha t} \right) d \xi \quad (\text{A.34})$$

where

I_0 = the modified Bessel function of the first kind and order zero

and

ξ = dummy variable of integration.

A.4.3.1 Superposition of the instantaneous solution

Slug injection of recharge water is not very practical, but the principle of superposition in time (McWhorter and Sunada, 1977) can be used to obtain more useful solutions. The total volume of recharge water can be divided up into a number of slugs to be injected at specified time intervals. If many injections are used, the solution will approximate continuous recharge. To superimpose, let

C_j = height of one cylinder of slug injected water

t_j = the time of the instantaneous injection.

The superposition of n slug injections can be expressed as

$$H = \sum_{j=1}^n C_j \left(\frac{1}{2\alpha(t-t_j)} \right) \int_0^a \xi \exp - \left(\frac{r^2 + \xi^2}{4\alpha(t-t_j)} \right) I_0 \left(\frac{r\xi}{2\alpha(t-t_j)} \right) d\xi . \quad (A.35)$$

A.4.3.2 Computer implementation of the instantaneous solution

Equation (A.34) is in integral form and must be transformed into an equation of summation form which can be numerically evaluated. Gaussian quadrature is a numerical integration technique which can be used to evaluate the integral. The integral must be transformed so that the range of integration varies between -1 and 1. To perform the transformation, let

$$\beta = \frac{2\xi}{a} - 1. \quad (A.36)$$

Then

$$\xi = (\beta + 1) \frac{a}{2} \quad (A.37)$$

and

$$d\xi = \frac{a}{2} d\beta. \quad (A.38)$$

Substitution of equations (A.37) and (A.38) into equation (A.34), and changing the limits of integration, yields

$$H = \frac{Ca^2}{8\alpha t} \int_{-1}^1 (\beta+1) \exp \left[\frac{r^2 + \left((\beta+1) \frac{a}{2} \right)^2}{4\alpha t} \right] I_0 \left[\frac{r(\beta+1)\frac{a}{2}}{4\alpha t} \right] d\beta. \quad (A.39)$$

where β = dummy variable of integration.

The integral is evaluated by Gaussian quadrature (Appendix G-1).

$$H = \frac{Ca^2}{8\alpha t} \sum_{i=1}^m (A_i+1) \exp \left[\frac{r^2 + \left((A_i+1) \frac{a}{2} \right)^2}{4\alpha t} \right] I_0 \left[\frac{r(A_i+1)\frac{a}{2}}{4\alpha t} \right] W_i \quad (A.40)$$

where

A_i = Gaussian quadrature abscissus

W_i = Gaussian quadrature weight factors

and

m = number of quadrature points.

To simulate continuous recharge, it is best to divide the recharge period into equal intervals and inject a slug of water at the beginning of each time interval. The height, C , of all the slug cylinders is found by dividing the total volume of recharged water (Rt) by the number of time intervals and the storage coefficient. Let

$$C_j = \frac{Rt}{Sn} \quad (A.41)$$

and

$$t_j = \frac{(j-1)t}{n} \quad (A.42)$$

Substituting for C_j and t_j in equation (A.35) and using Gaussian quadrature to evaluate the integral yields

$$H = \frac{Rt}{Sn} \frac{a^2}{8\alpha} \sum_{j=1}^n \frac{1}{(t-t_j)} \sum_{i=1}^m (A_i+1) \exp^{-\left[\frac{r^2 + \left((A_i+1) \frac{a}{2} \right)^2}{4\alpha(t-t_j)} \right]} I_0 \left[\frac{r(A_i+1)a}{4\alpha(t-t_j)} \right] \cdot W_i \quad (\text{A.43})$$

The Bessel function is evaluated by a polynomial approximation (Appendix C-4).

A.4.4 Continuous Solution

Integration of the instantaneous solution for a circular basin over time (equation (A.34)) yields a continuous solution. The continuous solution involves two integrals but is still easily evaluated on a computer.

For a constant rate of recharge, R , C is given by

$$C = \int_0^t \frac{R}{S} d\tau \quad (\text{A.44})$$

Substitution for C , and integration equation (A.34) with respect to time yields

$$H = \frac{R}{2\alpha S} \int_0^t \frac{1}{\tau} \int_0^a \xi \exp^{-\left[\frac{r^2 + \xi^2}{4\alpha\tau} \right]} I_0 \left[\frac{r\xi}{2\alpha\tau} \right] d\xi d\tau \quad (\text{A.45})$$

which is the continuous solution for recharge from a circular basin.

A.4.4.1 Solution at the basin center

At the basin center, $r = 0$ and $I_0(0) = 0$. Equation (A.45) reduces to

$$H_0 = \frac{R}{2\alpha S} \int_0^t \frac{1}{\tau} \int_0^a \xi \exp\left(-\frac{\xi^2}{4\alpha\tau}\right) d\xi d\tau, \quad (\text{A.46})$$

where H_0 = mound height at the basin center.

To integrate the inner integral, let

$$w = \frac{\xi^2}{4\alpha\tau}. \quad (\text{A.47})$$

Then

$$d\xi = \frac{1}{2w^{1/2}} (4\alpha\tau)^{1/2} dw \quad (\text{A.48})$$

With this transformation (eq. A.47 and A.48) equation (A.46) becomes

$$H = \frac{R}{S} \int_0^t \int_0^{\frac{a^2}{4\alpha\tau}} e^{-w} dw. \quad (\text{A.49})$$

which upon integration is

$$H = \frac{R}{S} \int_0^t \left(1 - \exp\left(-\frac{a^2}{4\alpha\tau}\right)\right) d\tau \quad (\text{A.50})$$

Let

$$u_0 = \frac{a^2}{4\alpha\tau} \quad (\text{A.51})$$

then

$$d\tau = -\frac{a^2 du}{4\alpha u^2} \quad (\text{A.52})$$

Substitution of equations (A.51) and (A.52) into equation (A.50) yields

$$H = \frac{Rt}{S} \left[1 - \frac{a^2}{4\alpha} \int_{u_0}^{\infty} \frac{e^{-u}}{u^2} du \right] \quad (\text{A.53})$$

where

$$u_0 = \frac{a^2}{4t} \quad (\text{A.54})$$

Integration by parts and rearrangement yields

$$h_0 = \frac{Rt}{S} \left(1 - e^{-u_0} + u_0 \int_{u_0}^{\infty} \frac{e^{-u}}{u} du \right) \quad (\text{A.55})$$

The remaining integral is the well function (McWhorter and Sunada, 1977).

This solution is exactly the same as the solution that Glover presents (1960). It is a very useful solution in that it can be easily solved by hand and requires no numerical integration because the well function can be found by polynomial approximations (Abramowitz and Stegun, 1972) or found in a table.

A.4.4.2 Computer implementation of the continuous solution for a circular basin.

The integral over time in equation (A.45) is also numerically integrated by Gaussian quadrature. Again the range of the integral must be from -1 to 1, so let

$$\lambda = \frac{2\tau}{t} - 1 \quad (\text{A.56})$$

then

$$d\tau = \frac{t}{2} d\lambda. \quad (\text{A.57})$$

With this transformation and with the transformation of the integral over space (eq. A.40) equation (A.45) becomes

$$H = \frac{R a^2}{16\alpha S} \int_{-1}^1 \frac{2}{(\lambda+1)t} \int_{-1}^1 (\beta+1) \exp \left[-\frac{r^2 + ((\beta+1)\frac{a}{2})^2}{2\alpha t(\lambda+1)} \right] I_0 \left[\frac{r(\beta+1)a}{2\alpha t(\lambda+1)} \right] dBd\lambda \quad (\text{A.58})$$

The equation can now be written in summation form, integrating by Gaussian quadrature with n points.

$$H = \frac{R a^2}{8\alpha St} \sum_{j=1}^m \frac{1}{(A_j+1)} \left\{ \sum_{i=1}^m (A_i+1) \exp \left[- \frac{r^2 + \left((A_i+1) \frac{a}{2} \right)^2}{2\alpha t (A_j+1)} \right] \right. \\ \left. I_0 \left[\frac{r(A_i+1)a}{4\alpha t (A_j+1)} \right] W_i \right\} W_j. \quad (\text{A.59})$$

The continuous solution requires far less computer time than superposition of instantaneous slug injections. In one instance it took 250 instantaneous slug injections for the solution to converge to the central mound height given by the continuous solution. This required about 25 times the computer time required by the continuous solution. For this reason the continuous solution was used in the comparison of solutions.

A.4.5 Glover's Continuous Solution for a Rectangular Basin

Glover's solution for a rectangular basin satisfies equation (A.29), the initial condition

$$H(x, y, 0) = 0 \quad (\text{A.60})$$

and boundary conditions

$$H(\infty, y, t) = 0 \quad (\text{A.61})$$

$$H(x, \infty, t) = 0. \quad (\text{A.62})$$

These conditions state that the initial water table is horizontal and that the mound height at an infinite distance from the basin center is zero at any time. The solution is

$$H = \frac{R}{S} \int_0^t \left(\frac{1}{\sqrt{\pi}} \int_{u_1}^{u_2} e^{-u^2} du \right) \left(\frac{1}{\sqrt{\pi}} \int_{u_3}^{u_4} e^{-u^2} du \right) d\tau \quad (\text{A.63})$$

$$\text{where } u_1 = \frac{(x - \frac{L}{2})}{d}, \quad u_2 = \frac{(x + \frac{L}{2})}{d}$$

$$u_3 = \frac{(y - \frac{L}{2})}{d}, \quad u_4 = \frac{(y + \frac{L}{2})}{d}$$

and

$$d = \sqrt{4\alpha(t - \tau)}.$$

From the definition of the error function (Appendix C-3) the solution can be written

$$H = \frac{Rt}{4S} \int_0^t (\text{erf } u_2 - \text{erf } u_1) (\text{erf } u_4 - \text{erf } u_3) d\tau. \quad (\text{A.64})$$

A.4.5.1 Computer implementation of Glover's solution for a rectangular basin.

Glover originally suggested that equation (A.64) be evaluated by Simpson's rule. It was found that Gaussian quadrature gives much better results than does Simpson's rule. Simpson's rule is presented as well as Gaussian quadrature to compare the different means of evaluation.

To use Simpson's rule, let

$$\xi = \frac{\tau}{t} \quad (\text{A.65})$$

With this transformation equation (A.64) becomes

$$H = \frac{Rt}{4} \int_0^1 (\operatorname{erf} u_2 - \operatorname{erf} u_1) (\operatorname{erf} u_4 - \operatorname{erf} u_3) d\xi \quad (\text{A.66})$$

with $d = \sqrt{4\alpha t(1 - \xi)}$.

In Simpson's rule, when $\xi = 1$, the denominator in each of the u terms goes to zero. When $x = \frac{L}{2}$ or $y = \frac{W}{2}$, the case arises when both numerator and denominator are zero. This leads to erroneous evaluation, especially near the edge of the basin. For example, consider points laying on the line $y = 0$, with x coordinate 199.5 and 200.5 with time = 30 days, $b = 200$, and other parameter values given in Table A.1. The height at $x = 199.5$ is 5.3 ft. and at $x = 200.5$ is 7.9 ft., indicating that there is a discontinuity near the boundary.

To numerically integrate by Gaussian quadrature, equation (A.64) must be transformed to obtain the proper form. Let

$$\omega = \frac{2\tau}{t} - 1 \quad (\text{A.67})$$

then

$$\tau = (\omega + 1) \frac{t}{2} \quad (\text{A.68})$$

and

$$d\tau = \frac{t}{2} d\omega. \quad (\text{A.69})$$

Changing the limits of integration, equation (A.64) is transformed to

$$H = \frac{Rt}{8} \int_{-1}^1 (\operatorname{erf} u_2 - \operatorname{erf} u_1) (\operatorname{erf} u_4 - \operatorname{erf} u_3) d\omega \quad (\text{A.70})$$

with

$$d = \sqrt{2\alpha t(1 - \omega)}$$

This is evaluated by Gaussian quadrature with n points as

$$H = \frac{Rt}{8} \sum_{i=1}^n (\operatorname{erf} u_2 - \operatorname{erf} u_1) (\operatorname{erf} u_4 - \operatorname{erf} u_3) W_i \quad (\text{A.71})$$

where

$$d = \sqrt{2\alpha t(1 - A_i)}$$

Figure A.4 gives a comparison of results obtained by Simpson's rule and Gaussian quadrature using $b = 200$ and the data from Table A.1. Gaussian quadrature gives a much smoother solution. At large times using Simpson's rule may lead to large errors.

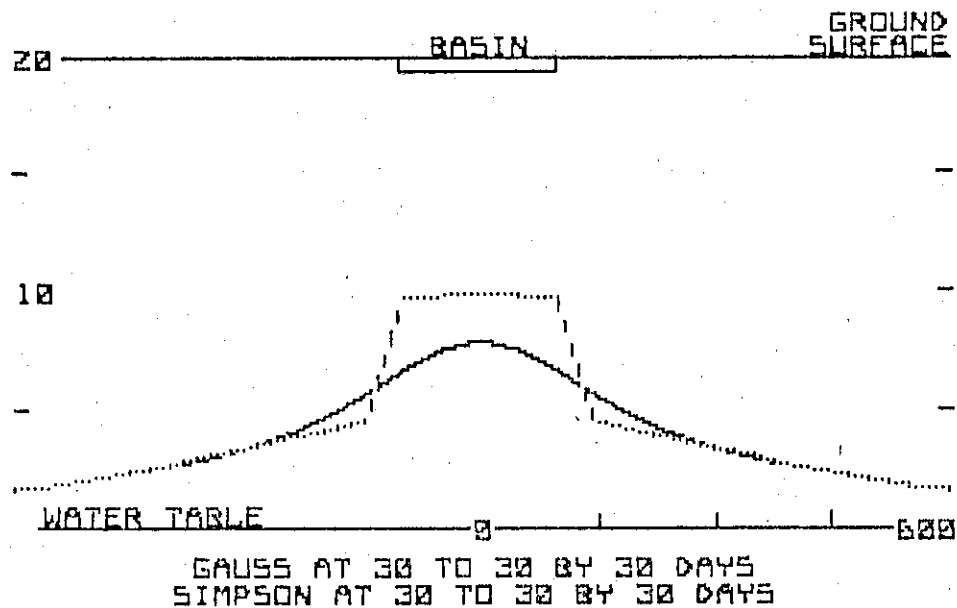


Figure A.4 - Simpson's rule (dotted line) and Gaussian quadrature (solid line) for integrating Glover's solution.

A.4.5.2 Superposition of Glover's solution in time

The principle of superposition in time (McWhorter and Sunada, 1977) can be used to obtain solutions with variable recharge rates. For example, consider recharge of a constant rate R occurring for a period t' then shutting off. To obtain a mound profile at times greater than

t' , the mound heights obtained for a period of $t - t'$ are subtracted from mound heights resulting from time period t (equation B.1). Figure A.5 gives an example of mound profiles at 30 and 60 days, with time of shutt off at 30 days (with $b = 200$ ft. and data from Table A.1). At 60 days, the mound heights near the center of the basin are too low. When the product of transmissivity and time is large, resulting in small arguments in the error function, equation(A.71) gives results which are less than the true solution. Preliminary studies show that Hantush's method (1967) for evaluating equation (A.64) does not introduce large errors at large times and transmissivities.

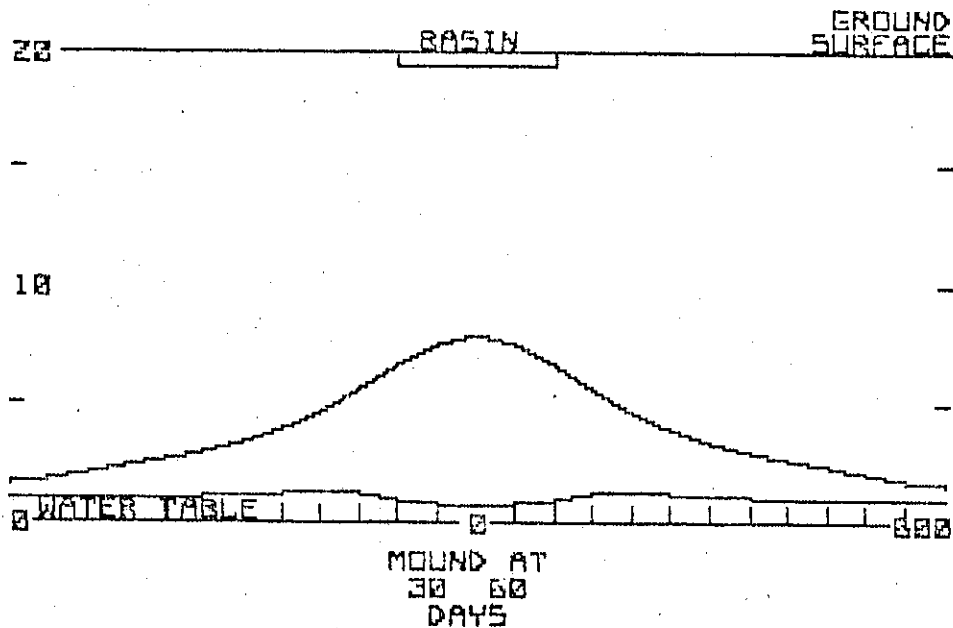


Figure A.5 - Mound profile at 30 and 60 days using Gaussian quadrature to evaluate Glover's solution for rectangular basins (eq. A.70).

A.5 Hantush's Solution for Circular and Rectangular Basins

Hantush (1967) presents solutions for recharge of a continuous rate from both circular and rectangular basins. The governing differential equation for groundwater flow (eq. A.10) was rearranged and solved by means of Laplace transforms. Hantush uses a different linearization technique than Glover which was found to give better results than Glover's linearizing technique when the mound rise is large compared to the initial saturated depth. It was shown that Hantush's solution for a rectangular basin is identical to Glover's solution and that Hantush's linearization can be applied to Glover's solutions.

A.5.1 Hantush's Approach: Rearrangement of the Governing Partial Differential Equation for Groundwater Flow.

To rearrange the non-linear Boussinesq equation (eq. A.10), Hantush introduces a new variable, Z. Let

$$Z = h^2 - b^2. \quad (\text{A.72})$$

Noting that

$$\frac{\partial}{\partial x} (h \partial h / \partial x) = \frac{1}{2} \frac{\partial^2 h^2}{\partial x^2}, \quad (\text{A.73})$$

substitution of equation (A.72) into equation (A.10) yields

$$\frac{\partial^2 Z}{\partial x^2} + \frac{\partial^2 Z}{\partial y^2} + \frac{2R}{K} = \frac{S}{2h} \frac{\partial Z}{\partial t}. \quad (\text{A.74})$$

The equation is still non-linear, so a linearization procedure must be applied.

A.5.2 Hantush's Linearization Technique.

To linearize, Hantush lets

$$h \approx \bar{b} = \frac{1}{2} (h(t) + b), \quad (\text{A.75})$$

where $h(t)$ is the calculated saturated thickness at the time and place of interest. This technique averages the initial saturated depth and the saturated depth at the time of interest to give a constant average transmissivity ($T = K\bar{b}$) at each point. Because $h(t)$ is not known, a priori, an iterative technique must be used to obtain numerical results from the equation.

A.5.3 Hantush's Solution for a Circular Basin

In radial coordinates equation (A.74) is written

$$\frac{\partial^2 Z}{\partial r^2} + \frac{1}{r} \frac{\partial Z}{\partial r} + \frac{2R}{K} = \frac{S}{K\bar{b}} \frac{\partial Z}{\partial t} \quad (\text{A.76})$$

The initial condition assumes a horizontal water table at $t = 0$, or

$$Z(r, 0) = 0. \quad (\text{A.77})$$

The boundary conditions are that the slope of the water table at the basin center is 0, and the mound heights at infinite distances away from the center are 0, or

$$\partial Z(0, t) / \partial r = 0 \quad (\text{A.78})$$

and

$$Z(\infty, t) = 0. \quad (\text{A.79})$$

The solution is

$$Z = \frac{2R}{a^2 K} \int_0^{\infty} \frac{(1 - \exp(-\frac{\beta^2}{u_0}))}{\beta^2} J_1(\beta) J_0\left(\frac{r}{a} \beta\right) d\beta \quad (\text{A.80})$$

where

$$u_o = \frac{a^2}{4\alpha t}$$

$$\alpha = K \bar{b}/S = T/S$$

and J_0 and J_1 are the zero and first ordered Bessel functions of the first kind.

A .5.3.1 Center basin mound height.

Under the basin center Hantush presents the solution

$$h_o^2 - b^2 = \frac{Ra^2}{2K} \left\{ W(u_o) + \frac{(1 - e^{-u_o})}{u_o} \right\} \quad (A.81)$$

where

h_o = saturated thickness at the basin center

$W(u_o)$ = well function of u .

This can be shown to be identical to Glover's solution for mound height at the center of a circular basin. Z is factored out to obtain

$$Z = h_o^2 - b^2 = (h_o + b) (h_o - b) = 2 \bar{b} H. \quad (A.82)$$

Dividing both sides of equation (A.82) by $2\bar{b}$ yields

$$H_o = \frac{Ra^2}{4bK} \left\{ W(u_o) + \frac{(1 - e^{-u_o})}{u_o} \right\}. \quad (A.83)$$

Multiplying and dividing the right hand side of equation (A.84) for S/t and rearranging noting that $u_o = a^2 S/4bKt$ yields

$$H_o = \frac{R}{S} \left\{ 1 - e^{-u_o} + u_o W(u_o) \right\} \quad (A.84)$$

which is exactly the same as Glover's solution (eq. A.55).

A.5.3.2 Approximate solutions to recharge from a circular basin.

Hantush also presents approximate solutions for mound height. These solutions provide a much easier means of numerical evaluation requiring less computer time but are subject to restrictions.

Let $u = r^2/4at$. For $u_1 \leq .05$, the mound height at any point under the basin can be approximated by

$$Z = \frac{R a^2}{2K} \left\{ W(u_0) - \left(\frac{r}{a}\right)^2 e^{-u_0} + \frac{1}{u_0} (1 - e^{-u_0}) \right\} \quad (\text{A.85})$$

for $r < a$.

Outside of the basin, for $u \geq 0.5$ the approximate solution is

$$Z = \frac{R a^2}{2K} \left\{ W(u) + 0.5 u_0 e^{-u} \right\} \quad (\text{A.86})$$

for $r \geq a$.

Neither approximate solution requires numerical evaluation.

A.5.3.3 Computer implementation of Hantush's solution for a circular basin.

The improper integral in eq. (A.80) is evaluated by LaGuerre integration (Appendix C-2); Abramowitz and Stegun, 1972). In n steps, using LaGuerre integration, eq. (A.80) takes the summation form of

$$Z = \frac{2R}{a^2 K} \sum_{i=1}^n \frac{W_i' e^{A_i'}}{(A_i')^2} \left(1 - \exp \left(-\frac{A_i'^2}{u} J_1(A_i') J_0\left(\frac{r}{a} A_i'\right) \right) \right) \quad (\text{A.87})$$

where

A_i' = abscissas of LaGuerre integration

and

W_i' = weights of LaGuerre integration.

The Bessel functions are evaluated by polynomial approximations (Appendices C-5 and C-6).

The saturated depth, h , is contained in Z and u , thus h appears on both sides of the equation. An iterative approach must be used to solve the equation. A first guess of $h_i = b$ goes into the right hand side of equation from which h is calculated. If $H \ll b$, then this first guess will give a very close solution for h . On the next iteration the calculated h is substituted for h_i on the right hand side of the equation. The process is repeated until $h \approx h_i$. A flow chart helps illustrate this procedure.

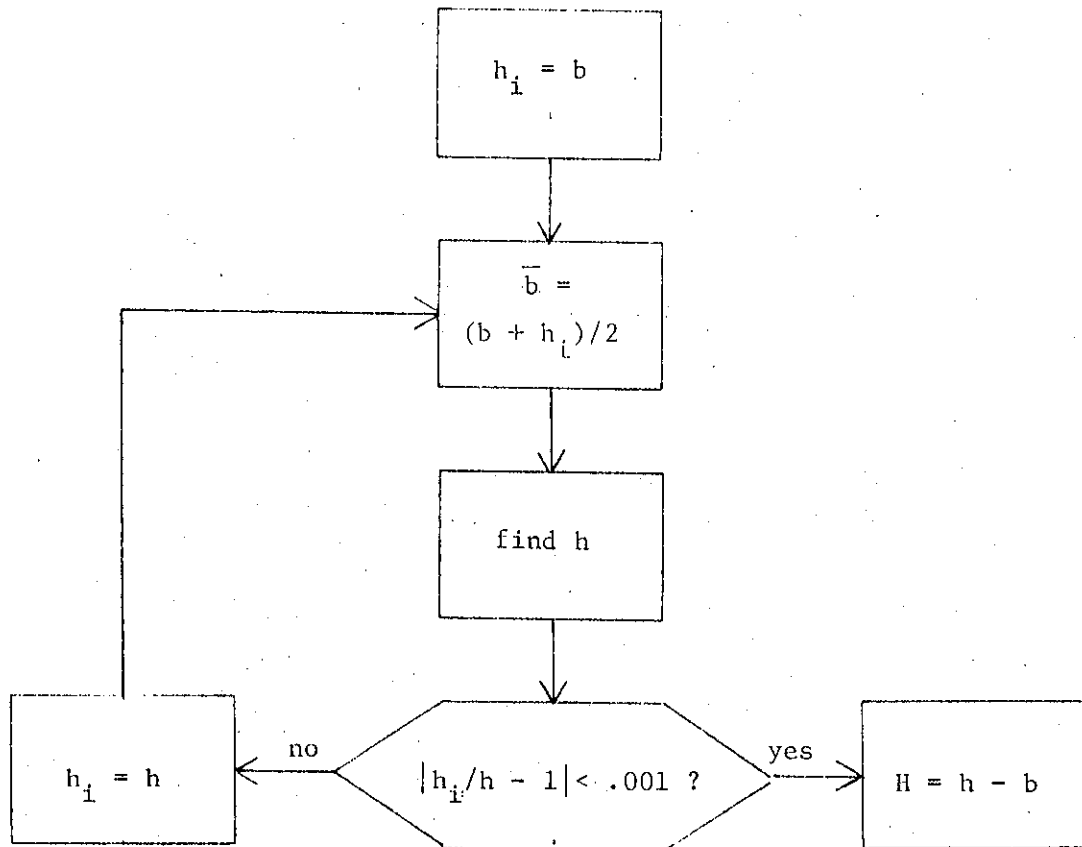


Figure A.6 - Iterative technique used with Hantush's linearization.

For problems where $h \gg b$, it takes 3 or 4 iterations to converge on a solution near the center of the basin and 2 iterations to converge at greater distances.

A.5.4 Hantush's Solution for a Rectangular Basin

Hantush solves the rearranged governing equation for groundwater flow (eq. A.74) along with his suggested linearization technique (eq. A.75) by the method of Laplace transforms to obtain a solution for a rectangular basin. The solution subject to the initial condition

$$Z(x,y,0) = 0 \quad (\text{A.88})$$

and boundary conditions

$$Z(0,y,t)/x = \partial Z(x,0,t)/\partial y = 0 \quad (\text{A.89})$$

$$Z(\infty,y,t)/x = \partial Z(x,\infty,t)/\partial y = 0$$

is

$$Z = \frac{\bar{R}b}{2S} \int_0^t \left[\operatorname{erf} \left(\frac{\frac{L}{2} + x}{d} \right) + \operatorname{erf} \left(\frac{\frac{L}{2} - x}{d} \right) \right] \left[\operatorname{erf} \left(\frac{\frac{W}{2} + y}{d} \right) + \operatorname{erf} \left(\frac{\frac{W}{2} - y}{d} \right) \right] d\tau \quad (\text{A.90})$$

where

$$d = \sqrt{4\alpha\tau}$$

and

$$\alpha = K \bar{b} / S$$

The solution is strikingly similar to Glover's solution (eq. A.64) and can be shown to be exactly the same. The only difference between Hantush's and Glover's solution for a rectangular basin is the linearization technique used.

A.5.4.1 Equivalence of Hantush's and Glover's solution for rectangular basin.

To show the equivalence of Hantush's and Glover's solution for rectangular basin, the relationship of $Z = 2 \bar{b} H$ from eq. (A.82) is used. The erf functions can also be rearranged by the fact that $\text{erf}(-x) = -\text{erf}(x)$ (Abramowitz and Stegun, 1972). With these two relationships, eq. (A.91) becomes

$$H = \frac{R}{4S} \int_0^t \left[\text{erf}\left(\frac{x + \frac{L}{2}}{d}\right) - \text{erf}\left(\frac{x - \frac{L}{2}}{d}\right) \right] \cdot \left[\text{erf}\left(\frac{y + \frac{W}{2}}{d}\right) + \text{erf}\left(\frac{y - \frac{W}{2}}{d}\right) \right] d\tau. \quad (\text{A.92})$$

Now the only difference with equation (A.92), and Glover's solution (eq. (A.64)) is the denominator, d , in the error functions. Let

$$\tau = t - \tau'. \quad (\text{A.93})$$

then

$$d = \sqrt{4\alpha(t - \tau')} \quad (\text{A.94})$$

and the variable of integration in equation (A.92) is changed to τ' . This shows that Hantush's and Glover's solution for rectangular basins are identical.

Because Hantush's solution is identical to Glover's solution for rectangular basins, Hantush's linearization procedure can be applied to Glover's solution. To modify Glover's solution (eq. A.64), simply replace $\alpha = T/S$ with $\alpha = K\bar{b}/S$ where \bar{b} is given by equation (A.75).

A.5.4.2 Computer implementation of Hantush's solution for a rectangular basin.

The method presented to evaluate the integral in Glover's solution (eq. A.64) is also used with Hantush's equation (see eq. A.67 through

A.71). As in the case of Hantush's solution for a circular basin, an iterative approach must be followed and is presented in the flowchart in Figure A.5.

A.6 Rao and Sarma's Solution for a Rectangular Basin

Using the same linearization technique as Hantush, Rao and Sarma (1981) present a solution to the recharge problem subject to finite boundary conditions. Although the solution they present looks easy to evaluate, it was found that excessive computer time is required to obtain accurate results.

A.6.1 Solution

Instead of requiring the mound rise to be zero at infinite distances away from the mound, Rao and Sarma impose an impermeable rectangular boundary around the basin. The rectangular boundary is of length $2M$ and with $2B$, with the respective boundaries parallel to the x and y axes and symmetric around the basin. Because of these impermeable boundaries, the slope of the water table at the boundaries is 0 which leads to the boundary condition

$$\frac{\partial Z}{\partial x}(M, y, t) = \frac{\partial Z}{\partial y}(x, B, t) = 0 \quad (\text{A.95})$$

The initial condition requires a horizontal water table at time = 0, or

$$Z(x, y, 0) = 0. \quad (\text{A.96})$$

Subject to these boundary and initial conditions equation (A.74) is solved to yield

$$\begin{aligned}
S = & \frac{8R}{K} \frac{A^2 B^2}{\pi^4} \left\{ \sum_{m=1}^{\infty} \sum_{n=1}^{\infty} \left[\frac{1}{mn} \frac{1}{m^2 M^2 + n^2 B^2} \right. \right. \\
& \left. \left. \left(1 - \exp \left(- \frac{K \bar{b} \pi^2}{S} [(m^2 M^2 + n^2 B^2)t / (M^2 B^2)] \right) \right) \right. \right. \\
& \left. \left. \sin \left(\frac{m\pi L}{2M} \right) \sin \left(\frac{n\pi W}{2B} \right) \cos \left(\frac{m\pi X}{M} \right) \cos \left(\frac{n\pi Y}{B} \right) \right] \right\} \\
& + \frac{R \bar{b} LW}{2MB} \cdot t
\end{aligned} \tag{A.97}$$

Although it may be difficult to match these symmetric boundary conditions to field situations, if M and B are large enough, an infinite aquifer can be simulated. Values $M = 50 L$ and $B = 50 W$ are suggested by Rao and Sarma and are used throughout this paper.

A.6.2 Computer Implementation of Rao and Sarma's Solution

To evaluate the infinite series, convergence criteria must be made. The summation is made to stop when the incremented value is a small percentage of the existing sum. A flow chart illustrates the procedure. Let SUM equal the summation value, χ equal the value to be added onto SUM and $conv.$ equal a convergence factor.

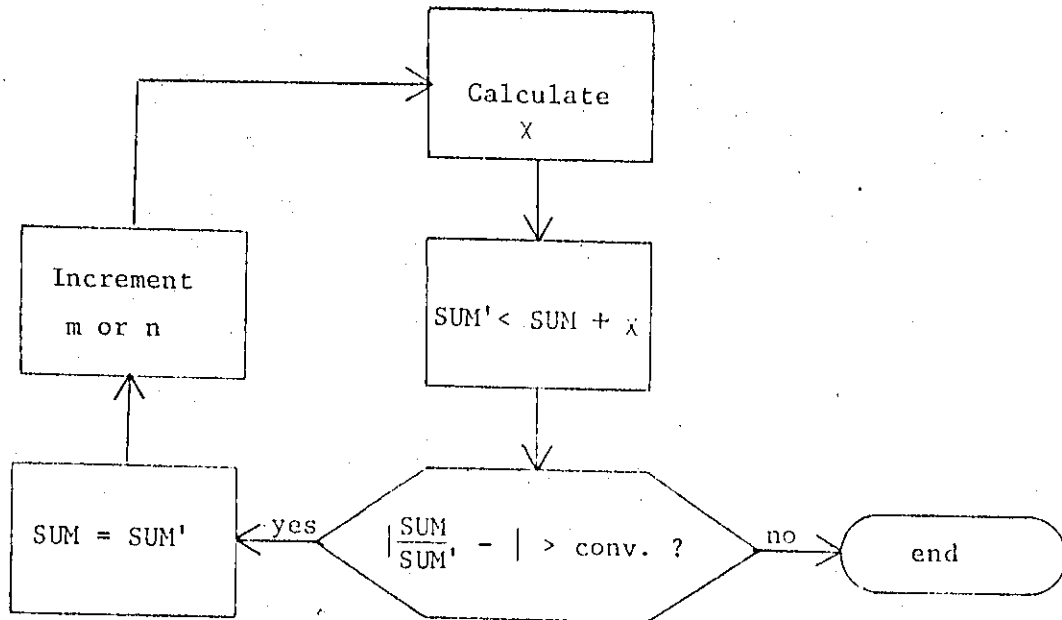


Figure A.7 - Convergence Criteria for Rao and Sarma's Solution.

Table A.2 illustrates the convergence with saturated depth equal to 2000, time equal 30 days, and values from Table A.1.

TABLE A.2 - Convergence of Sarma and Rao's Solution

<u>Conv.</u>	<u>Mound Height (ft)</u>
.1	1.87
.01	5.50
.005	6.33
.001	7.19
.0005	7.29
.00001	7.35

Convergence of the infinite series is slow because the numerator as well as the denominator increases with increasing m and n . A convergence factor of .001 is used in the rest of this paper, as a trade off between accuracy and computer time requirements.

A.7 Hunt's Solution for a Circular Basin

Hunt (1971) argues that the vertical velocities near the free surface of a recharge mound cannot be neglected, thus the Dupuit Forchheimer assumption cannot be used. He solves the Laplace equation in radial coordinate for the case of recharge from a circular basin subject to a linearized boundary condition for the free surface.

A.7.1 Hunt's Solution

Hunt uses the differential equation for a confined aquifer (for the derivation, see McWhorter and Sunada, 1977, or Bear, 1980). Because specific storage which describes storage in terms of expansion of water or contraction of the aquifer skeleton is negligible in an unconfined aquifer, the term for specific storage is set to zero. The governing differential equation for groundwater flow is derived without the Dupuit Forchheimer assumptions and is the Laplace equation

$$\frac{\partial^2 h}{\partial r^2} + \frac{1}{r} \frac{\partial h}{\partial r} = 0 \quad (\text{A.98})$$

The nonlinearity and transient characteristics of artificial recharge appear in the boundary conditions.

One boundary condition is at the free surface. Let

$$\phi = -K h = -K \left(\frac{P}{\rho g} + z \right). \quad (\text{A.99})$$

At the free surface, the pressure is atmospheric ($P = 0$), so

$$\phi(r, \eta, t) = -K z \quad (\text{A.100})$$

where η is the z coordinate at the free surface. Differentiating equation (A.100) with respect to time gives

$$\frac{\partial \phi}{\partial r} \frac{dr}{dt} + \left(\frac{\partial \phi}{\partial z} + K \right) \frac{dz}{dt} + \frac{\partial \phi}{\partial t} = 0. \quad (\text{A.101})$$

The velocities dx/dt and dz/dt can be written

$$\frac{dr}{dt} = \frac{1}{S} \frac{\partial \phi}{\partial r} \quad (\text{A.102})$$

$$\frac{dz}{dt} = \frac{1}{S} \left(\frac{\partial \phi}{\partial z} + K \right) \quad (\text{A.103})$$

Equation (A.101) becomes

$$\left(\frac{\partial \phi}{\partial r} \right)^2 + \left(\frac{\partial \phi}{\partial z} + K \right) \left(\frac{\partial \phi}{\partial z} + K \right) + S \frac{\partial \phi}{\partial t} = 0 \quad (\text{A.104})$$

which is the non-linear free surface boundary condition. To linearize, Hunt first defines dimensionless variables

$$\phi^* = \frac{\phi}{Ka}, \quad r^* = \frac{r}{a}, \quad b^* = \frac{b}{r}$$

$$z^* = \frac{z}{a}, \quad t^* = \frac{Kt}{Sa}$$

$$R^* = \frac{R}{K}, \quad \eta^* = \frac{\eta}{r}$$

He assumes solutions for ϕ^* of the form

$$\phi^* = \phi_1^* R^* + \phi_2^* (R^*)^2 + \dots \quad (\text{A.105})$$

As a linearizing approximation only the first order term, $\phi_1^* R^*$ is kept. After substituting the dimensionless forms into the non-linear free surface boundary condition (eq. A.104) and neglecting any higher order terms the boundary condition becomes linearized.

$$\begin{aligned} \left(\frac{\partial}{\partial z^*} + \frac{\partial}{\partial t^*} \right) \phi_1^* (r^*, b^*, t^*) &= 1 \quad (r^* < 1) \\ &= 0 \quad (|r^*| > 1) \end{aligned} \quad (\text{A.106})$$

The Laplace equation in radial coordinates in dimensionless form is expressed

$$\frac{\partial^2 \phi^*}{\partial r^2} + \frac{1}{r} \frac{\partial \phi^*}{\partial r} = 0 \quad (\text{A.107})$$

The remaining boundary conditions are that the base of the aquifer is impermeable and that the initial water surface is horizontal or

$$\frac{\partial \phi_1^* (r^*, 0, t^*)}{\partial z^*} = 0 \quad (\text{A.108})$$

$$\phi_1^* (r^*, z^*, 0) = 0 \quad (\text{A.109})$$

The solution to this boundary valued problem is

$$\frac{z^*}{R^*} = \int_0^{\infty} \frac{J_0(\gamma r^*) J_1(\gamma)}{\gamma} \left(\frac{1 - \exp(-\gamma t^* \tanh(\gamma b^*))}{\tanh(\gamma b^*)} \right) d\gamma \quad (\text{A.110})$$

where γ is the dummy variable of integration.

For an infinitely deep aquifer ($b^* \rightarrow \infty$) the solution is

$$\frac{z^*}{R^*} = \int_0^{\infty} \frac{J_0(\gamma r^*) J_1(\gamma)}{\gamma} [1 - \exp(-\gamma t^*)] d\gamma \quad (\text{A.111})$$

Equation (A.111) is used in the method of evaluation suggested by Hunt

where the improper integral is transformed to a finite integral.

$$\frac{z^*}{R^*} - \left(\frac{z^*}{R^*} \right)_{b^* \rightarrow \infty} = \int_0^{n/b^*} \frac{J_0(\gamma r^*) J_1(\gamma)}{\gamma} G(\gamma, t^*, b^*) d\gamma + \Delta \quad (\text{A.112})$$

where

$$G(\gamma, t^*, b^*) = \frac{1 - \exp(-\gamma t^*) \tanh(\gamma b^*)}{\tanh(\gamma b^*)} - 1 + \exp(-\gamma t^*) \quad (\text{A.113})$$

and

$$\Delta \leq 4 \left(\frac{b^*}{n} \right)^{\frac{1}{2}} (\coth(n) - 1) \quad (\text{A.114})$$

where

n = an arbitrary number large enough to keep Δ small.

A.7.2 Computer Implementation of Hunt's Solution

Because the Bessel functions used in equation (A.110) change signs with different arguments, the integral is difficult to evaluate. Hunt's suggested method of breaking the equation into a finity integral plus the solution as the saturated depth goes to infinite is used (eq.(A.112)).

First, n must be found to keep the error Δ in equation (A.112) small. An error of $\Delta < .01$ keeps error less than .1% of the calculated mound height in the trials used. n is first chosen as 3 and equation (A.114) used to the maximum calculate Δ . If Δ is greater than .01, n is incremented and Δ recalculated until the error becomes sufficiently small.

The integral in equation (A.112) is transformed to be evaluated by Gaussian quadrature. Let

$$\omega = \frac{2\gamma - 1}{n/b^*} \quad (\text{A.115})$$

and

$$\beta = (\omega + 1) \frac{n}{2b^*} \quad (\text{A.116})$$

Equation (A.112) becomes

$$\frac{z^*}{R^*} - \left(\frac{z^*}{R^*}\right)_{b^* \rightarrow \infty} = \frac{n}{2b^*} \int_{-1}^1 \frac{J_0(\beta r^*) J_1(\beta)}{\beta} G(\beta, t^*, b^*) d\omega + \Delta \quad (\text{A.117})$$

The semi-infinite integral in equation (A.111) is evaluated by LaGuerre integration (Appendix C-2). In summation form the dimensionless solution is

$$\frac{z^*}{R^*} = \frac{n}{2b^*} \sum_{i=1}^m \frac{J_0(\beta r^*) J_1(\beta)}{\beta} \frac{1 - \exp(-\beta t^*) \tanh(\beta b^*)}{\tanh(\beta b^*)} - 1 + \exp(\beta t^*) \cdot W_i + \quad (\text{A.118})$$

$$\sum_{j=1}^n \frac{J_0(A_j' r^*) J_1(A_j')}{A_j'} [1 - \exp(-A_j' t^*)] * W_j' + \Delta$$

The Bessel functions are evaluated by polynomial approximations (Appendices C-5 and C-6). Δ is neglected and the mound height is found by introducing the dimensioned variables.

$$H = \frac{z^*}{R^*} \cdot \frac{rR}{K} \quad (\text{A.119})$$

Even with the modifications suggested by Hunt the evaluation of the solution at great distances away from the center of the basin is difficult. Figure A-8 shows the mound profile obtained by using ten integration steps. At distance far away from the recharge basin edge the solution oscillates due to the difficult integration of the Bessel functions.

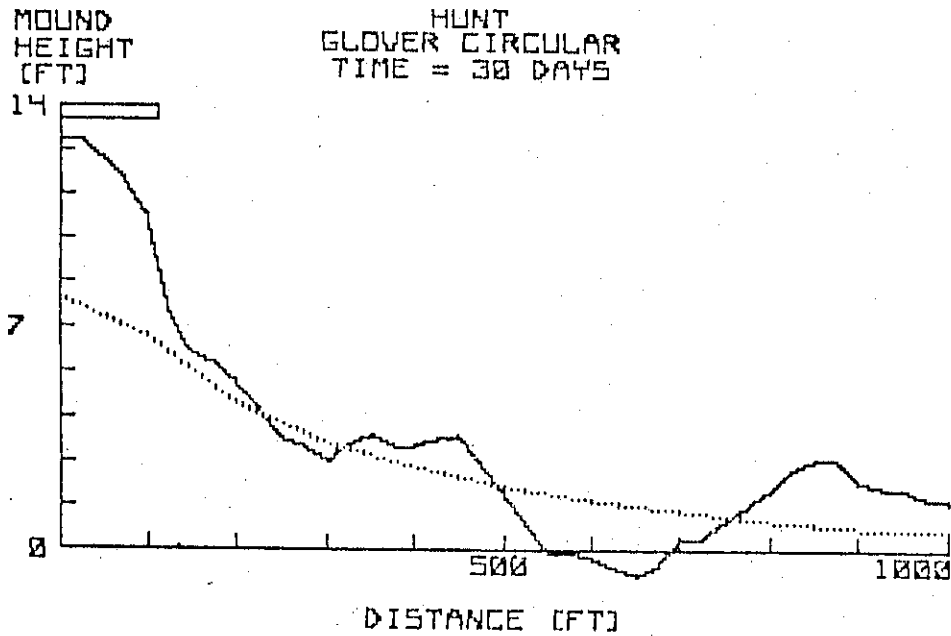


Figure A.8 - Hunt's Solution (solid line) and Glover's Solution
($b = 200$ ft., $t = 30$ days).

A.8 Finite Element Program

In the comparison of various solutions of the artificial recharge problem, a finite element program was used as a numerical solution. The results obtained from this method are considered an accurate representation of an actual field situation. The results provide a base line for comparing the analytical solutions.

The program, written and programmed by Dr. James Warner at Colorado State University, uses the Galerkin finite element technique with

triangular elements and linear shape function to simulate two-dimensional groundwater flow (Warner, 1981). In its most general form, the method solves the non-linear Boussinesq equation for a non-homogeneous, isotropic medium (eq. A.9). The boundary conditions are finite and can be placed where desired by the user. The initial conditions do not require a horizontal water table at the initial time.

As initial conditions all of the analytical solutions require a horizontal water table at the beginning time. Each analytical solution, except for Rao and Sarma's, uses an aquifer of infinite areal extent. To simulate these conditions in the finite element method, an equal initial value of head is given to all the nodes. The infinite boundary conditions are simulated by moving the aquifer boundaries far enough away that they do not influence the solution:

Because most of the interest is in the area of recharge, the grid for the recharge site uses many elements in this zone (Fig. A.9). The elements further away from this zone become larger and larger. Because of symmetry, only one fourth of the problem is modelled. The boundaries starting at the edge of the basin are path lines where no flow crosses. A total of 460 elements and 268 nodes are used.

To get a solution at a desired time, the solution is updated at several intermediate time steps. The first time step is input into the model by the user, always kept at 1000 seconds for the results obtained in this paper. The time is incremented by

$$t_{n+1} = f \cdot t_n \quad (\text{A.120})$$

where

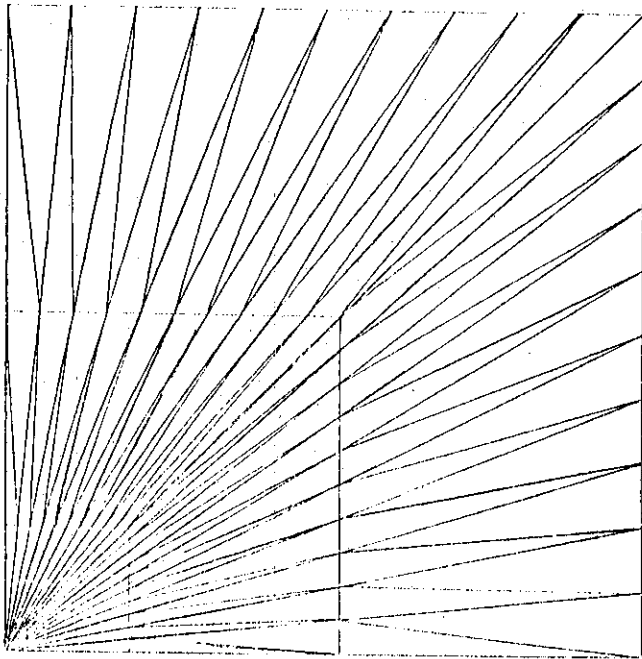
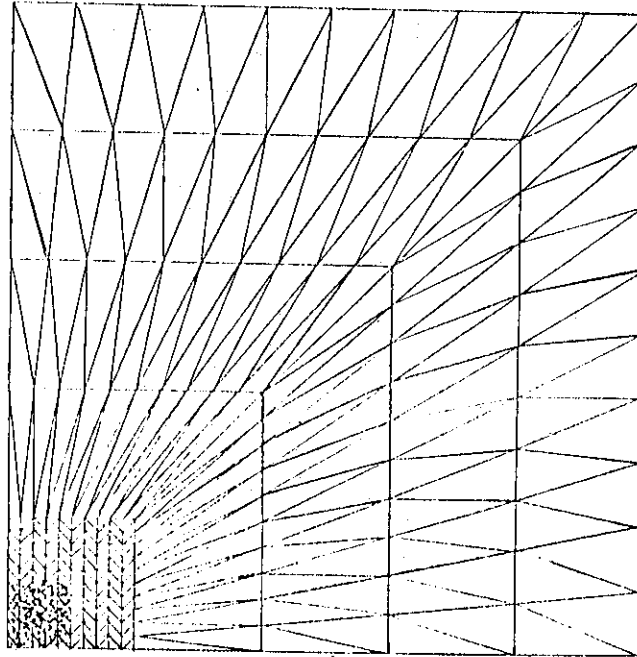


Figure A.9 - Finite Element Grid for Comparing Solutions. The shaded area represents the recharge basin.

t_{n+1} = time at next time step

t_n = time at present time step

f = multiplication factor (= 1.5)

until t_{n+1} is greater than or equal to the desired time.

To simulate the non-linear flow problem of an unconfined aquifer, transmissivity must change with time. After a value for head is calculated at a time step for a node, it is used in updating the transmissivity at that node for the next time step by

$$T_{n+1} = K(b + (h_n - b)) \quad (\text{A.121})$$

where

T_{n+1} = transmissivity at the next time step

b = initial saturated thickness

h_n = head at present time step

If many time steps are used, this approximation should be good in updating transmissivity.

For a confined aquifer, the transmissivity is constant in time and given by $T = Kb$. This is the same as the linearization procedure used by Glover. In the following comparisons, the solution for unconfined aquifers was used.

A.9 Comparison of Solutions

To give a good comparison of solutions, the accuracy and computer time of each solution were studied. A program, written in Fortran V containing all analytical solutions was used as well as the finite element program. First an optimal number of integration steps was determined. Next, the computer time requirement of each solution

technique was compared. The solutions for square and circular basins were contrasted. To check the linearization assumptions, the initial saturated depth was varied. The solutions were then compared to field data collected by Bianchi and Haskell (1975).

To actually determine the "best" solution, considerable amounts of experimental data are needed which are not available. Even though an ideal solution cannot be determined, some conclusions can be reached on the applicability of the various solutions.

A.9.1 Determination of Integration Steps

Most of the equations used require numerical integration. The optimal number of integration steps is difficult to determine analytically and may change for different problems. What is desired is a number of steps which will give reliable results for all problems.

A trial and error procedure was used to try and determine this number. For Gaussian quadrature 5, 7, 10 and 20 point quadrature were tried. For LaGuerre quadrature 5 and 10 steps were used. The data from Table 2.1 was used with time equal 30 days keeping all inputs constant except for the initial saturated depth (b).

The mound height at the center of the basin is most sensitive to the number of integration steps. The values for center mound heights at 30 days with varying integration steps are shown in Table A.3. Both Glover and Hantush give closed form solutions for mound height at the center of the basin using the well function (eq. A.55 and A.81). These results, as well as results from the finite element model, should help in determining the number of integration steps.

TABLE A.3 - Solutions Obtained with Differing Integration Steps.

Mound Height at Basin Center ($t = 30$ days)						
integration steps	5	7	10	20	eq. (2.55) or eq. (2.81)	finite element
b(ft)						
Glover's Rectangular					eq. (2.53)	(con-fined)
20	43.42	43.32	42.91	42.94	42.22	39.81
50	22.62	23.04	22.90	22.80	22.94	21.16
200	6.78	7.39	7.80	7.91	7.91	7.40
1000	1.43	1.61	1.79	2.05	2.09	1.71
Glover's Circular					eq. (2.53)	(con-fined)
20	43.80	43.32	43.22	43.26	42.22	39.81
50	22.78	23.21	23.04	22.90	22.94	21.16
200	6.80	7.42	7.84	7.94	7.90	7.41
1000	1.43	1.61	1.79	2.05	2.09	1.71
Hantusch's Rectangular					eq. (2.80)	(uncon-fined)
20	29.72	29.76	29.56	29.55	29.70	27.85
50	19.61	20.10	20.07	19.95	20.06	18.72
200	6.67	7.27	7.68	7.79	7.79	7.29
1000	1.43	1.61	1.79	2.04	2.09	1.71
Hantusch's Circular					eq. (2.80)	(uncon-fined)
20	28.73		29.74		29.70	27.85
50	20.30		19.71		20.06	18.72
200	9.33		7.79		7.79	7.29
1000	2.21		2.44		2.09	1.71
Hunt						
20	62.48	53.44	44.61	46.38		
50	25.25	23.69	24.33	24.29		
200	12.84	12.02	12.82	12.82		
1000	11.20	11.12	8.65	10.43		

For the smaller values of initial saturated depth the results are very close, independent of integration steps. For larger initial saturated depth the values increase with increasing integration steps. The closed form solution of Glover and Hantush suggest that 10 or 20 steps is best in this case.

Hunt's solution and Hantush's solution for circular basins require LaGuerre integration. It appears that 10 steps are necessary to make the integration more stable.

In the following comparisons 10 integration steps were used in all cases.

A.9.2 Computer Time Requirements

To calculate the average length of computer time required for the calculation of one point, a subroutine provided by the Cyber 720 was used. After all the inputs and preliminary calculations are completed, the timer starts. Upon completion of calculation of points the timer stops, giving the time required to calculate the points. It was attempted to code each solution technique in an equally efficient manner into Fortran.

The time comparison was made with the data from Table A.1, using 30 days and a saturated depth of 200 ft. Eleven points were calculated at this time step for each solution technique except for Rao and Sarma's where one point was calculated. An average time per point was determined and normalized by dividing through by the fastest solution (Table A.4).

TABLE A.4 - Computer Time Requirements on the Cyber 720.

	Bauman	Glover Circ.	Glover Rect.	Hantush Rect.	Hantush Circ.	Hunt	Rao and Sarma
Time per Point (sec)	.006	.0506	.0155	.0289	.0255	.0293	8.662
Normalized	1	8.43	2.58	4.82	4.25	4.88	1437.0

These values may change with different data inputs due to varying numbers of iterations or preliminary calculations. This technique does, however, give a good representation of the computer time required by each solution technique.

Baumann's method is the fastest because it uses straightforward substitution and outside of finding the radius of influence (D), no iterations are used. Glover's rectangular solution is second because only one numerical integration is required per point. Both of Hantush's methods are of almost equal speed. They do not require iterations and, thus, take more time than Glover's method. Hunt's method requires two numerical integrations and takes approximately the same amount of time as Hantush's method. Glover's circular solutions requires two numerical integrations, one nested inside the other, and is thus relatively slow. Rao and Sarma's technique, due to poor convergence of two infinite series, requires by far the most time.

If Hantush's linearization is applied to Glover's rectangular method, about .0259 seconds per point is required. This is slightly faster than Hantush's rectangular procedure.

Because Rao and Sarma's technique takes so much time, it will not be considered in further analysis. It is assumed that if the boundaries are at a great enough distance, this method converges to the results obtained by Hantush's rectangular solution, since it is derived from the same differential equation.

A.9.3 Rectangular vs. Circular Basin.

In the literature it is often stated rectangular and circular basins of equivalent areas will have approximately the same solutions for mound heights given equivalent data inputs (Glover, 1960; Bittinger and Trelease, 1965; Bianchi and Haskell, 1968). This fact, if true, can be used advantageously. If only the mound height at the center is desired, the relatively simple equations of Glover and Hantush (eq. A.55 and A.81) can be used by transforming the area of a rectangular basin to that of a circular basin. Baumann and Hunt's solutions could be used to describe a rectangular basin. On the other hand, it could be advantageous to transform the area of a circular basin or other irregular shape into that of a square, allowing the use of solutions for rectangular basins.

To test this hypothesis, Glover's solution for a circular basin was used with a radius of 200 ft. and initial saturated depth of 200 feet and the rest of the data from Table 2.1. Four rectangular basins of equivalent areas, with width equal to 1, 1.5, 2 and 3 times the length were compared against the mound profile for a circular basin. The mound profiles for the rectangular basin passes through the corners where deviations of solutions are the greatest.

Figure A.10 compares the solutions for circular and rectangular basins. The circular and square solutions are almost identical. Small deviations occur with the width equal to twice the length.

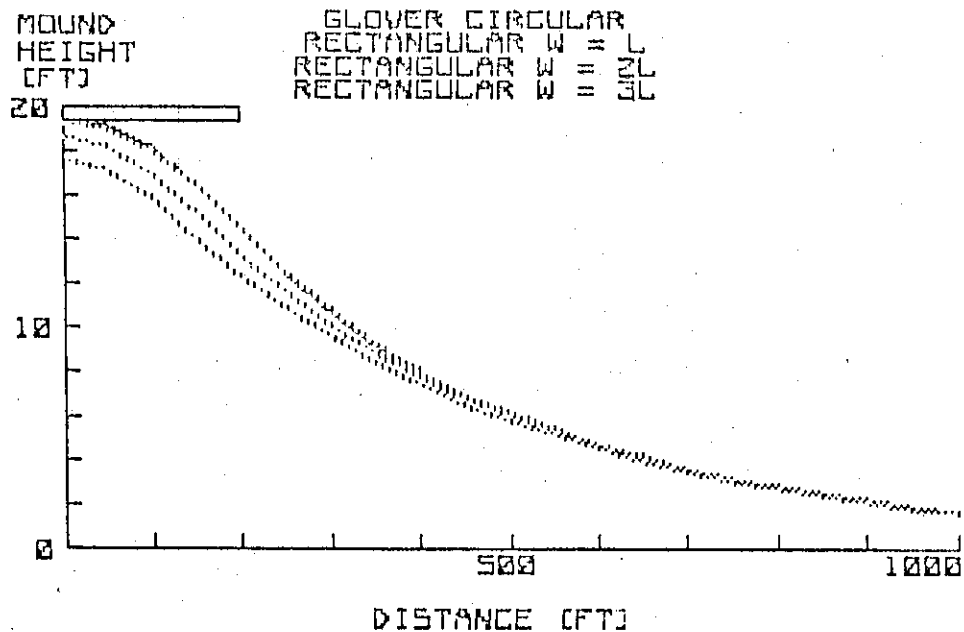


Figure A.10 - Rectangular vs. Circular Basin. A circular basin of radius 200 ft. (solid line) is compared with rectangular basins of equal areas (dotted line). The square basin ($W = L$) mound profile almost completely overlaps the circular basin.

Because the results for square and circular basins are so close, Glover's and Hantush's solutions for circular basins will be omitted in the remaining comparisons. It is also valid to compare Baumann and Hunt's solutions to those obtained with square basins.

A.9.4 Solutions with Varying Initial Saturated Depths

One of the stipulations of using the linearization technique of Glover is that the mound height be small compared to saturated depth. Hantush's linearization procedure may be used for smaller saturated depths. Baumann and Hunt do not use the Dupuit Forchheimer assumption and do not have to make this type of linearizing assumption. The finite element technique is assumed to give a good solution to the non-linear problem and will be used in the comparison of the different techniques.

The data used is from Table A-1, with two different initial saturated depths of 50 and 200 ft. For these two cases, the mound height at the center of the basin is plotted against time (Figs. A.11 and A.12) and the mound profile is plotted at 30 days (Figs. A.13 and A.14). The mound profile obtained using Hunt's solution is plotted until it begins to oscillate.

At an initial saturated depth of 200 ft., the mound height obtained by Glover's solution is about 4% of the saturated depth. There is not a large difference between Glover's, Hantush's and the finite element solution showing that Glover's linearization is valid in this case. Baumann's solution shows a greater mound height than these, especially at smaller times. Near the basin, Hunt's solution yields significantly greater values than any of the other techniques.

At an initial saturated depth of 50 feet the mound height obtained by Glover's solution is about 45% of the original saturated depth. In this case, Glover's solution deviates more from the finite element solution. Hantush's solution is close to the finite element solution

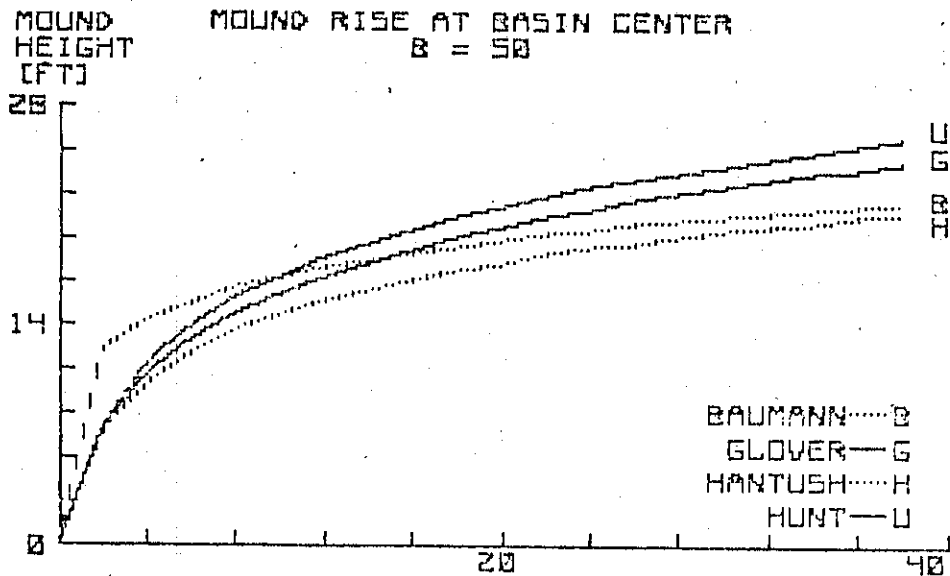


Figure A.11 - Mound rise at basin center vs. time ($b = 50$ ft; $t = 30$ days).

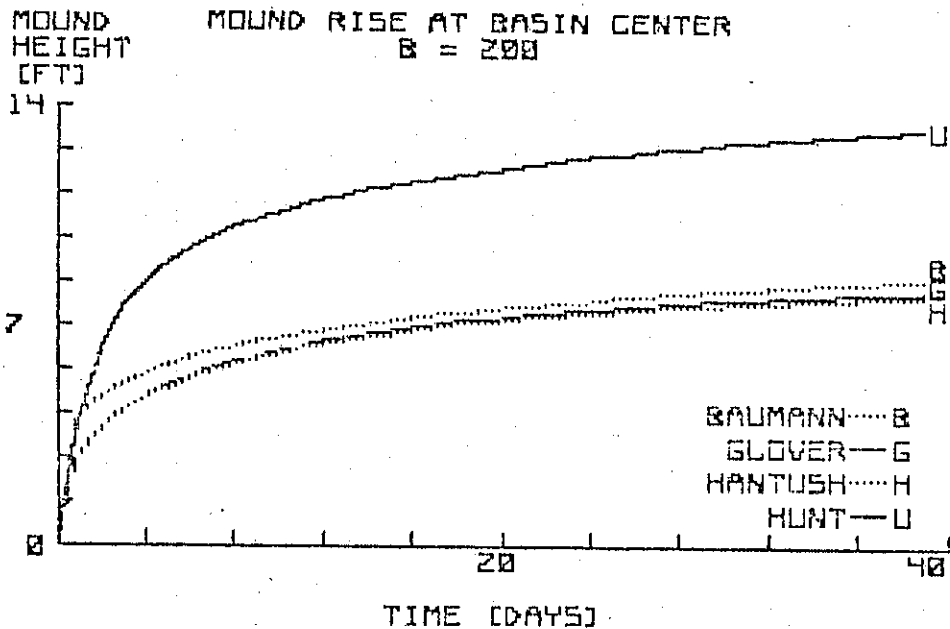


Figure A.12 - Mound rise at basin center vs. time ($b = 200$, $t = 30$ days).

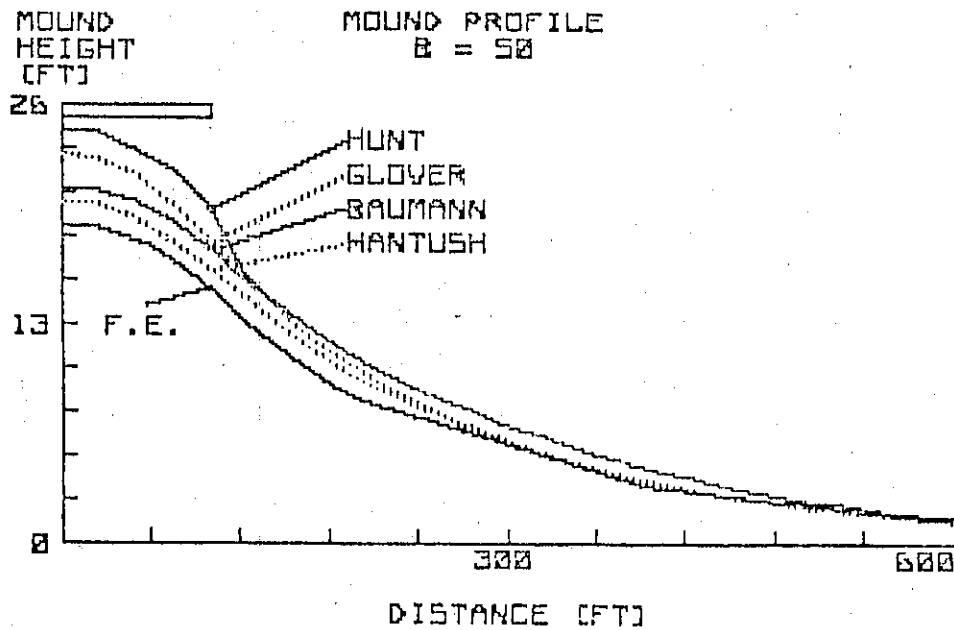


Figure A.13 - Mound profile ($b = 50$, $t = 30$ days).

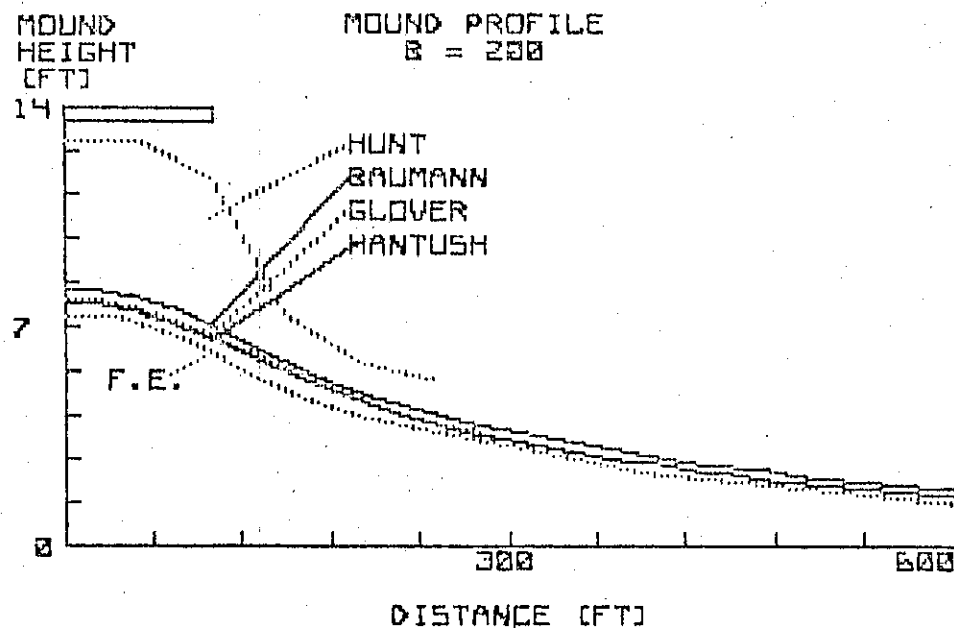


Figure A.14 - Mound profile ($b = 200$, $t = 30$ days).

showing that his linearization is valid in this case. Baumann's method yields the highest results at small times, but approaches Hantush's solution at larger times, showing that his method comes close to simulating the non-linear problem at larger times. Hunt's method in this case is close to Glover's solution.

A.9.5 Comparison with Field Experiment

Bianchi and Haskell (1968, 1975) conducted field tests of artificial recharge to measure the shape of a rising and declining recharge mound. Figure A.15 compares the experimental results with the analytical solutions at A.1 and 8.9 days. The analytical solutions do a fair job in predicting the mound profile. Hunt's method seems to do the best job in predicting the curvature of the mound.

Figure A.16 shows the experimental central mound heights changing with time, compared to the results obtained by analytical solutions. Again, the predicted values provide a fair match with observed values. None of the analytical solutions seem better than the other in this case. At small times, Bianchi and Haskell report air entrapped beneath the wetting front causing curvature of the advancing front. For this reason, the assumption of constant recharge rate is violated at small times and there is great deviation of the measured and predicted results.

A.10 Summary

A.10.1 Baumann's Solution

Baumann's method appears to be reliable at large times. The advantages of this method are that the equations are simple to solve

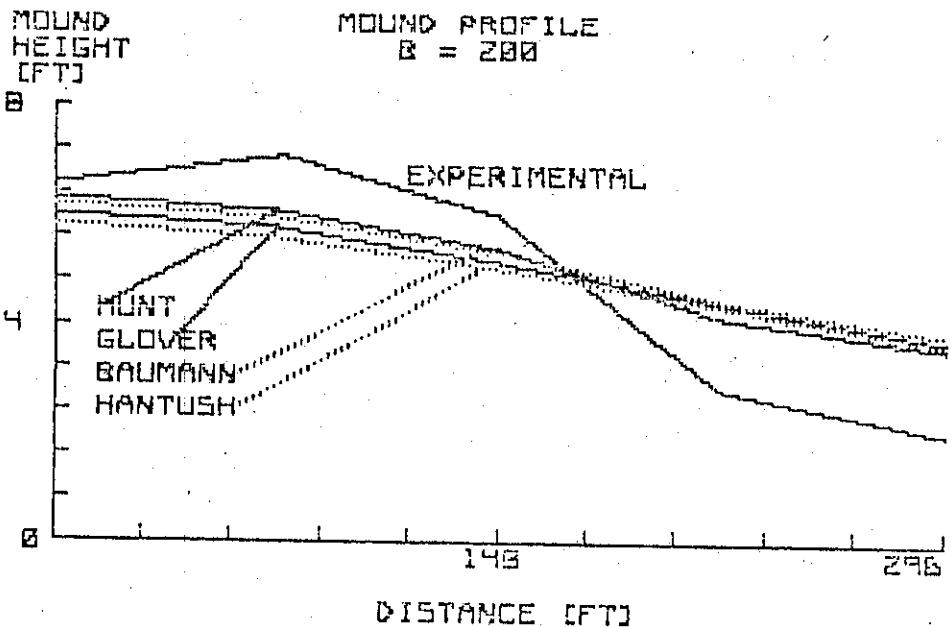


Figure A.15 - Mound profile obtained from field observations and from analytical solutions.

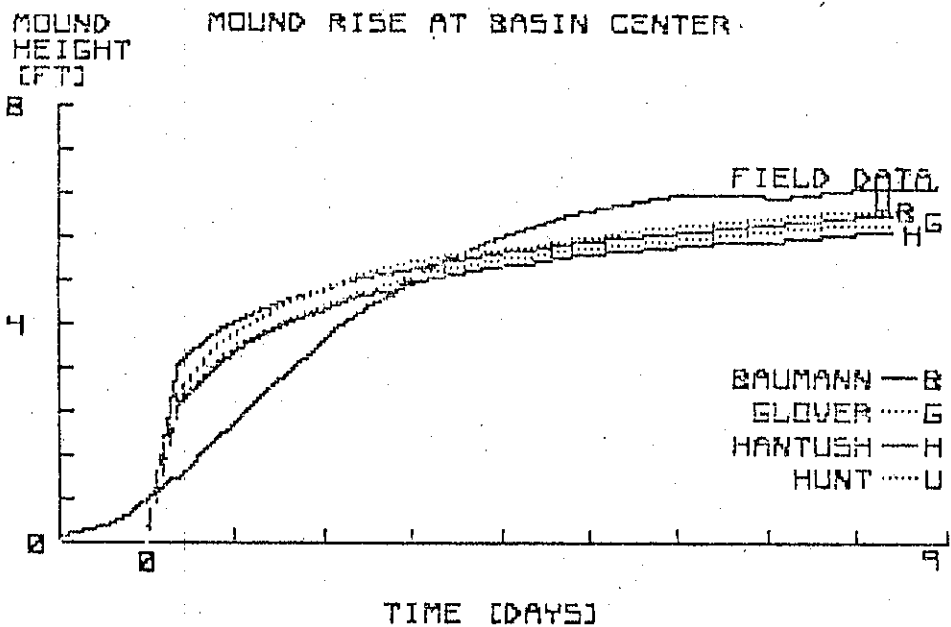


Figure A.16 - Mound rise at basin center vs. time from field observations and analytical solutions.

and can be done by hand. If a computer is used, the time requirements are very small. A misconception exists that Baumann's equation is valid only for steady state conditions because time does not appear explicitly in the equations. Using the method developed in this study, Baumann's equation can be applied to the transient case. However, at small times there may be error in this method.

A.10.2 Glover's Solutions

A.10.2.1 Circular basin solution

Glover's solution for a circular basin using superposition of slug injections is much slower than the rectangular basin solution of Glover and Hantush. The Glover circular solution for continuous recharge developed in this study is much faster than the method of superposition of slug injections but still takes about twice as much computer time as Glover's solution for a rectangular basin.

A.10.2.2 Rectangular basin solution

Glover's solution for a rectangular basin is relatively fast and has the advantage that only transmissivity is needed in the solution instead of both hydraulic conductivity and saturated depth. The linearization technique of Glover is valid only when mound rise is small compared to the initial saturated thickness. If Hantush's linearization procedure is applied to Glover's solution, the solution is valid when the mound rise is large compared to the initial saturated depth. With Hantush's linearization procedure both hydraulic conductivity and saturated depth are required.

A.10.3 Hantush's Solution

A.10.3.1 Rectangular basin

The linearization technique used by Hantush comes closer to simulating the non-linear problem of large mound rise compared to saturated depth than the technique used by Glover. Hantush's solution for a rectangular basin is identical to Glover's solution.

A.10.3.2 Circular basin

Hantush's circular solution is evaluated faster than Glover's circular solution, but appears more sensitive to the amount of integration steps. Both Hantush and Glover present solutions for rise at the basin center due to continuous recharge, which were shown to be identical. These solutions for the rise at the basin center are fast and easy to evaluate and are very close to the rise at the center of a square basin.

A.10.4 Rao and Sarma's Solution

Due to slow convergence of infinite series, Rao and Sarma's method uses an excessive amount of computer time.

A.10.5 Hunt's Solution

Hunt's method may be a valid description of artificial recharge, but this must be further verified by experiment. For complete analysis of the mound profile, this method should be avoided because of the difficult evaluation of the integral equation unless a better means of evaluation is found.

A.10.6 Numerical Solution

The finite element method has several advantages and should be used when the assumptions for the analytical solutions are severely violated. If the field situation is close to the ideal situation required by the analytical solutions or there is not enough available data for the finite element method, there is no advantage to this numerical technique to warrant the time required for analysis.

A.10.7 Suggested Analytical Methods

Either Glover's or Hantush's solutions for rectangular basins should be used for complete analysis of artificial recharge. If the aquifer has a large saturated depth compared to mound rise, Glover's method should be used for speed. If the mound height is larger either method with the linearization technique of Hantush should be used. Equations A.55) and A.81) provide excellent means for calculating mound height at the center of the basin.

APPENDIX B

MICROCOMPUTER MODEL OF ARTIFICIAL RECHARGE

B.1 Introduction

Recently a number of relatively inexpensive microcomputers have become available which can be effectively used by groundwater hydrologists to solve relatively complex groundwater problems. Though there are many engineering programs available for large main frame computers, there are very few available for microcomputers. The analytical solutions for artificial recharge do not require the high speed and storage offered by main frame computers and can be easily programmed on a microcomputer.

The program presented is a model of artificial recharge, designed for use on the APPLE II + 48 K microcomputer. Glover's solution for a rectangular basin and the principle of superposition are used to model the growth and decline of a recharge mound in the cases of an infinite, homogeneous aquifer and for a stream aquifer system. Results of the model are displayed graphically and numerically. The model can also be used to calculate discharge from the recharge basin into a stream for various times along the length of the stream. The program is totally interactive allowing for easy data input and a variety of output. The language used is APPLESOFT, the basic language adapted for the APPLE II + 48 K and APPLE II + 68 K microcomputers.

A similar model could be written for a main frame computer but there are many reasons for using a microcomputer. The program was developed as part of a demonstration of artificial recharge in the San Luis Valley in cooperation with the local irrigation districts. During the early stages of the project it became readily apparent that a need exists to transfer the complex mathematical equations into results that can be easily understood by water users. The graphics and interactive capabilities make microcomputers well suited for this transfer of knowledge. The program is extremely user friendly and can be used by both technical and non-technical people.

Another advantage of microcomputers is their low price. An APPLE II + 48 K microcomputer with a monitor and one disk drive can now be purchased for less than \$2,000.00 giving the owner a great deal of computational power and accessibility at a relatively inexpensive price. In addition, there has been an abundance of business oriented software developed which make microcomputers a valuable asset for moderately sized consulting firms (Dallaire, 1982; Butall, 1982). After the initial purchase only paper, disks for data storage and electricity must be paid for making run time very cheap.

A great advantage of hand held calculators is their portability. With a battery pack, microcomputers are also portable and can be taken into the field, an advantage not available with main frame computers.

The main disadvantage of microcomputers are their slow execution speed and storage. Unless the program is extremely large, disk utilization can usually provide enough storage. The Cyber 720 is approximately

1000 times faster than the APPLE II + microcomputer. Advances in microcomputer technology are rapidly increasing the speed and storage capabilities of microcomputers.

Two versions of the program were prepared, one written in APPLESOFT for the APPLE II + 48 K microcomputer and a compiled version for use on the APPLE + 64 K microcomputer. The compiled version operates about 1.5 times faster but requires more storage than the APPLESOFT version. The fully documented APPLESOFT program is presented in Appendix B.

B.2 Use of Glover's Solution

Glover's solution was chosen because it gives reliable results for many applications, it is easy to program, and is one of the fastest solutions. Baumann's solution requires less computer time but does not give reliable results for small times. For most conditions Hantush's solution and Glover's solution give approximately the same results and for small saturated depths Hantush's solution gives better results. However, Hantush's solution requires at least twice the computer time and both saturated depth and hydraulic conductivity must be known. It is more common to know only aquifer transmissivity which is the only aquifer parameter needed by Glover's solution.

B.2.1 Use of Superposition

The principle of superposition (McWhorter and Sunada, 1970) is used to obtain further solutions for finite aquifers and variable recharge. Superposition in time is used to calculate the decline of

the recharge mound after the end of the recharge period. With a stream in the vicinity, superposition in space is used to calculate mound profile and discharge to the stream with time.

At the end of the recharge period an image basin at the same location as the real basin begins withdrawal (negative R) while the real basin continues to recharge. The mound height due to the real basin is added to the drawdown due to the discharging image basin to give the actual mound height:

$$H = H_r + H_{it} \quad (B.1)$$

where

H_r = mound height contribution from the real basin,

H_{it} = mound height contribution from the image basin superimposed in time.

If a stream is in the vicinity, an image discharging basin is set up on the opposite side of the stream equidistant from the real basin (Fig. B-1). The drawdown from the image basin is superimposed onto the mound height contribution from the real basin to give the actual mound height

$$H = H_r + H_{is} \quad (B.2)$$

where

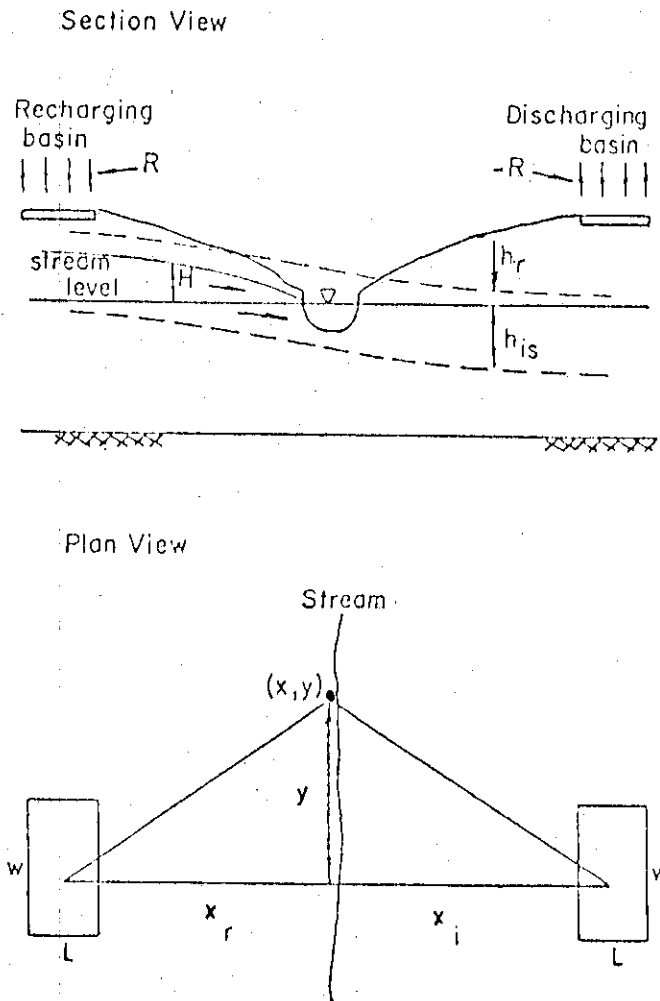


Figure B.1 - Definition sketch of artificial recharge with a stream.

H_{is} = drawdown contribution from the image basin superimposed in space.

If the end of the recharge period has been reached and a stream is in the vicinity, an image basin at the same location as the real basin begins discharging and another image basin at the same location as the image basin opposite the stream begins recharging. The mound height at a selected location is given by

$$H = H_r + H_{is} + H_{it} + H_{its} \quad (B.3)$$

where

H_{its} = mound height contribution from the image basin superimposed in time and space.

B.2.2 Discharge to the Stream

The integral equation for flow to a stream is

$$Q_T = \int_{-\infty}^{\infty} \left(T \frac{dh}{dx} \right) dy \quad (B.4)$$

where

Q_T = total discharge to the stream, and

$T \frac{dh}{dx}$ = the discharge to the stream per unit length at a selected location along the stream (McWhorter and Sunada, 1977).

The integral is evaluated numerically by computing the integrand at selected intervals along the stream and integrating the distribution by the method of trapezoids (Fig. B.2) The numerical evaluation yields the expression for discharge

$$Q_T = 2 \sum_{i=1}^n \left[\frac{\left(T \frac{\partial h}{\partial x} \right)_{i+1} + \left(T \frac{\partial h}{\partial x} \right)_i}{2} \right] \Delta y_i \quad (B.5)$$

where

Δy_i = the interval between points $i-1$ and i along the length of the stream.

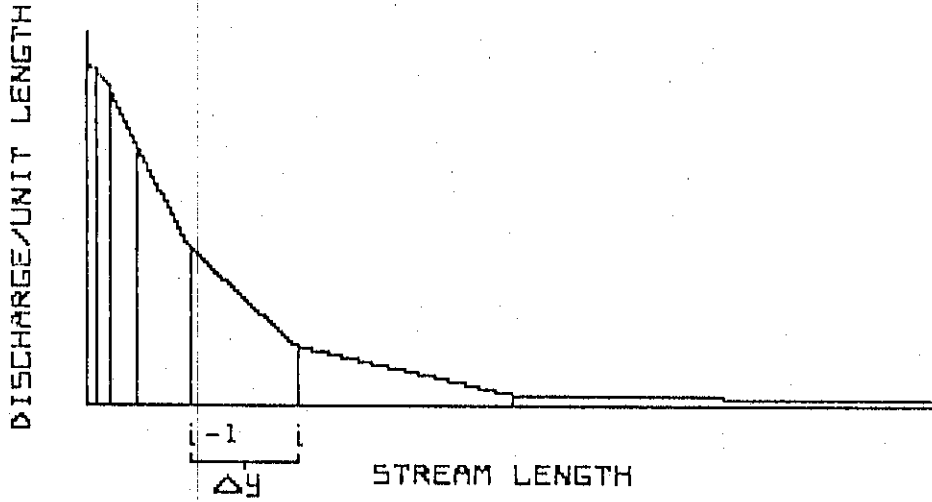


Figure B.2 - Method of trapezoids to obtain discharge to the stream.

The quantity $\frac{\partial h}{\partial x}$ is approximated by computing the head at 1 foot away from the stream (Fig. B.1). Since the head at the stream is constant and known (selected to be zero in this case) the term $\frac{\partial h}{\partial x}$ is approximated by

$$\frac{\partial h}{\partial x} \approx \frac{h^1 - 0}{1} = h^1. \quad (\text{B.6})$$

The integral equation becomes

$$Q_T = -T \sum_{i=1}^n [h_{i-1}^1 + h_i^1] \Delta y_i. \quad (\text{B.7})$$

If the end of the recharge period has reached, eq. (B.3) is used to calculate h_i^1 . Figure B.3 is a plot of discharge to the stream vs. time, with value obtained from the program using the data in Fig. B.3 below.

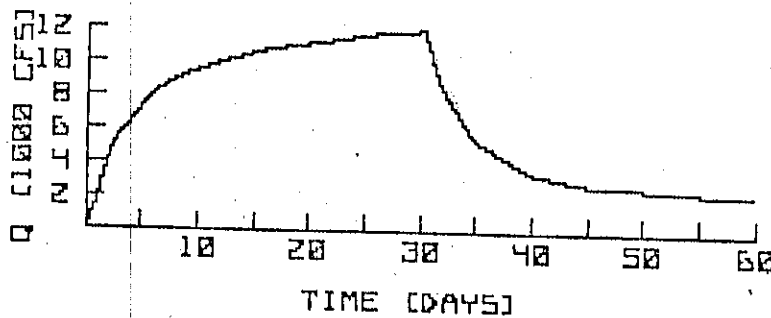


Figure B.3 - Discharge to the stream vs. time.

B.3 Program Description

Taking full advantage of the capabilities of the microcomputer, this interactive program is written to be self-explanatory and easy to manipulate. The graphics are employed for quick visual study. An example run is described to demonstrate the flow of the program. The figures represent what would be shown on the screen.

When starting the program, a menu presents a selection of model options (Fig. B.4). For this example, option 1 is chosen to model artificial recharge with a stream in the vicinity.

```
ARTIFICIAL RECHARGE

OPTIONS

1) STREAM IN VICINITY
2) NO STREAM IN VICINITY
3) READ FILES
4) EXIT

TYPE THE NUMBER OF YOUR CHOICE 1
```

Figure B.4 - Screen Display: model options. Artificial recharge is modeled with a stream in the vicinity.

The recharge parameters and their values are displayed on the screen (Fig. B.5). To change a value, the number corresponding to the recharge parameter to be changed is typed.

1)	RECHARGE RATE (FT/DAY)	1.5
2)	TRANSMISSIVITY (SQ. FT/DAY)	1000
3)	SPECIFIC YIELD	.15
4)	BEGINNING TIME (DAYS)	30
	FINAL TIME (DAYS)	30
	TIME INCREMENT (DAYS)	30
5)	END OF RECHARGE PERIOD (DAYS)	30
6)	BEGINNING DISTANCE (FT)	0
	FINAL DISTANCE (FT)	500
	DISTANCE INCREMENT (FT)	50
7)	DEPTH TO WATER (FT)	20
8)	BASIN WIDTH (FT)	100
9)	BASIN LENGTH (FT)	100
10)	ANGLE FROM LENGTH AXIS (DEG)	0
11)	DISTANCE TO STREAM	200
12)	CALCULATE MOUND PROFILE	YES
13)	CALCULATE DISCHARGE TO STREAM	YES

TYPE THE NUMBER OF THE VARIABLE YOU WISH TO CHANGE. TYPE 0 IF YOU WISH TO CONTINUE WITHOUT CHANGING.

Figure B.5 - Screen Display: parameter display. The depth to water is changed.

The old value is displayed and the user asked to input a new value (Fig. B.6). The updated parameter list is again displayed and the process repeated until the appropriate values are inputted by the user.

When 0 is typed the program checks for any value which is out of range. For an out of range error, the user will be told the mistake and asked to enter an appropriate value. With no mistakes, the program begins execution.

In this case, both mound profile and discharge to the stream are calculated. As values for head are calculated they are plotted on the graphics screen with the values of time, distance and mound height shown beneath the plot (Fig. B.7). Upon completion of the plot the

DEPTH TO WATER = 20 FEET

INPUT NEW DEPTH TO WATER 15

Figure B.6 - Screen Display: the depth is changed from 20 to 15 feet.

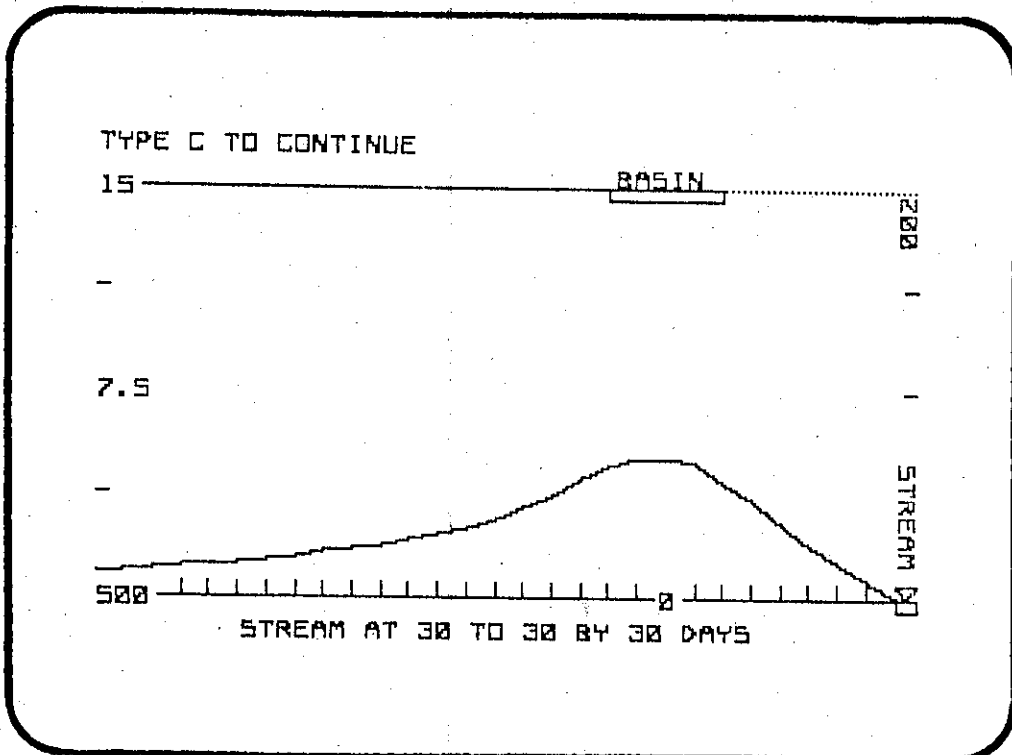


Figure B.7 - Screen Display: mound profile at 30 days.

user is asked to type C to continue. The graphics screen is then cleared and discharge to the stream is calculated. The display gives the distance along the stream, the mound height at one foot away from the stream and the discharge per unit length at that point as the points are calculated (Fig. B.8). When the discharge per unit length becomes negligible, the total discharge to the stream is given.

DISCHARGE TO STREAM		
DISTANCE ALONG STREAM (FT)	HEAD AT 1 FOOT (FT)	DISCHARGE/ UNIT LENGTH (SQ. FT./DAY)
30 DAYS		
0	.02263	22.63
25	.02218	22.18
50	.02095	20.95
100	.01719	17.19
200	.01045	10.45
400	3.74E-03	3.74
800	6E-04	.6
1600	1E-05	.01
3200	0	0
TOTAL DISCHARGE = 11000 CUBIC FT./DAY		

Figure B.8 - Screen Display: discharge to the stream at 30 days.

To reexamine and study the problem, the user is presented with a variety of output options (Fig. B.9). The "data display" option gives a list of the recharge parameters used. The "results display" tabulates the numerical values of the results. A hard copy of the data and results can be obtained with the "results printout" option. The graphics are

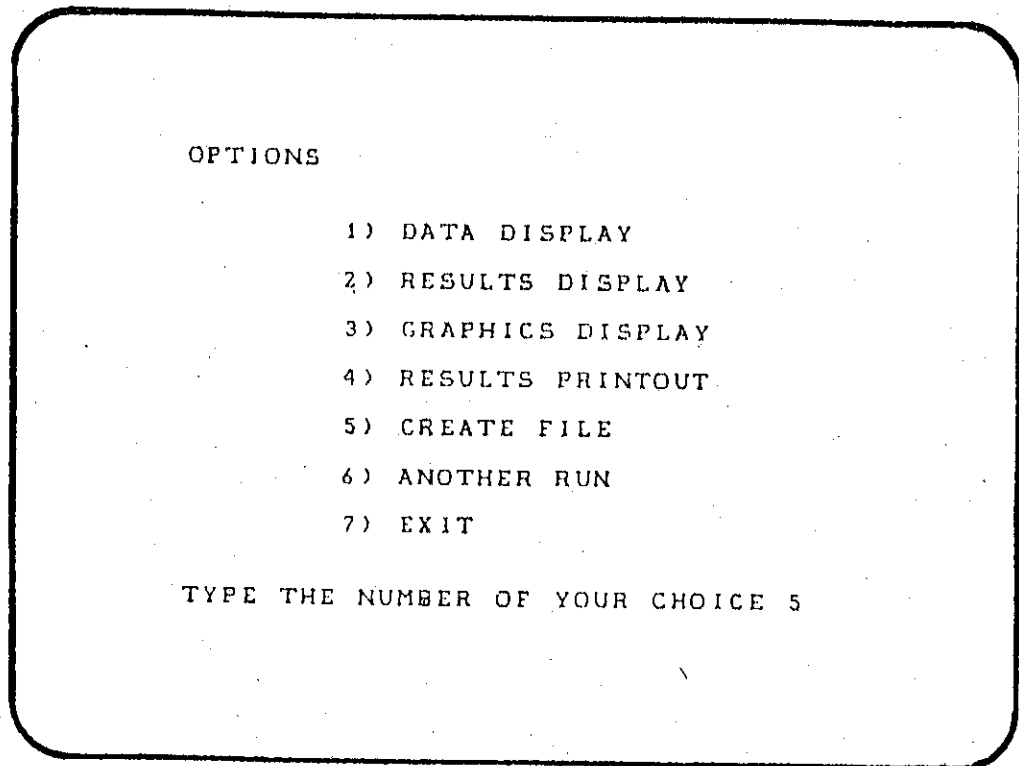


Figure B.9 - Screen Display: output options. Create file is chosen to store data and results on the disk.

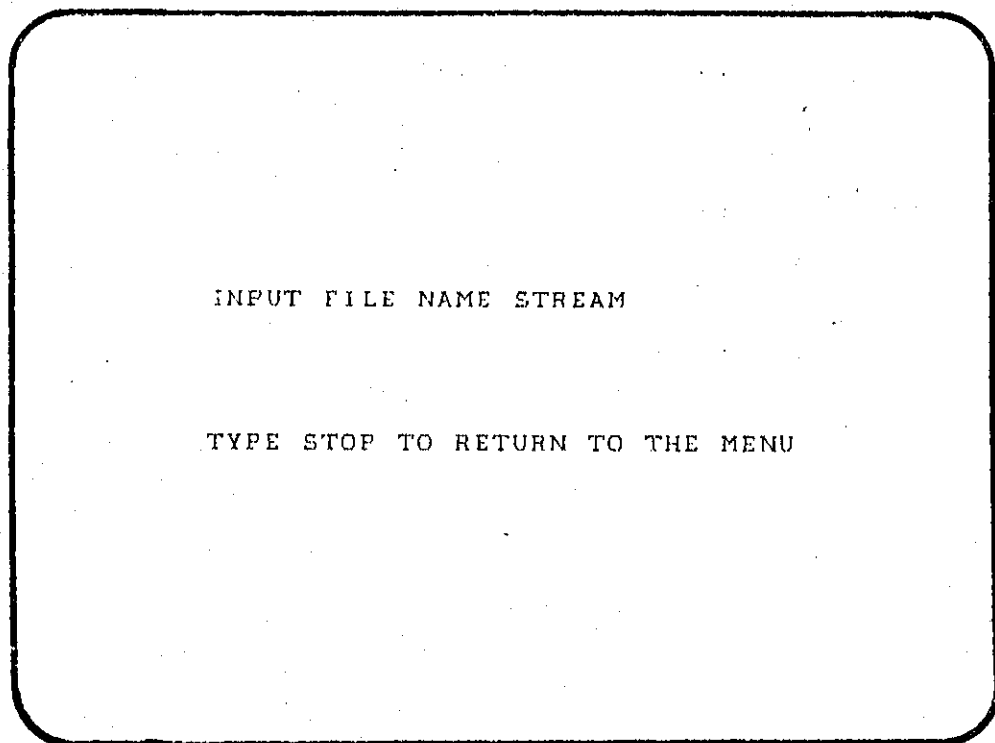


Figure B.10 - Screen Display: create files. The name "Stream" is given to the input data and results calculated.

quickly recreated by the "graphics display" option. Data and results can be stored on the disk with the "create file" option. The "another run" option allows the user to go back to the original model option, retaining all the present values of the recharge parameters. The "create files" option is chosen and the name given to the file is "stream" (Fig. B.10).

Next, the "another run" option is chosen and the original recharge option appears (Fig. B-4). "Read files" is then selected and the name of the file to be read is entered (Fig. B.11).

```
READ FILES
DO YOU WISH TO SEE THE CATALOG
(Y/ES,N/O)? N

INPUT FILE NAME NO STREAM

TYPE STOP TO RETURN TO THE MENU.
```

Figure B.11 - Screen Display: read files. The file "No Stream" is read from the disk.

The previously made file "no stream" is read from the disk. This file has exactly the same recharge parameters as "stream" but simulates recharge in an infinite aquifer. After the file has been read, the list of output option again appears on the screen with the exception that "creat file" has been changed to "read another file". Up to ten files can be read and simultaneously stored in memory. "Read another file" is chosen to read in the file "stream".

To compare the influence of a stream, the graphics will demonstrate any difference in mound profile. The "graphics display" option is chosen. The program asks which file is to be plotted (Fig. B.12).

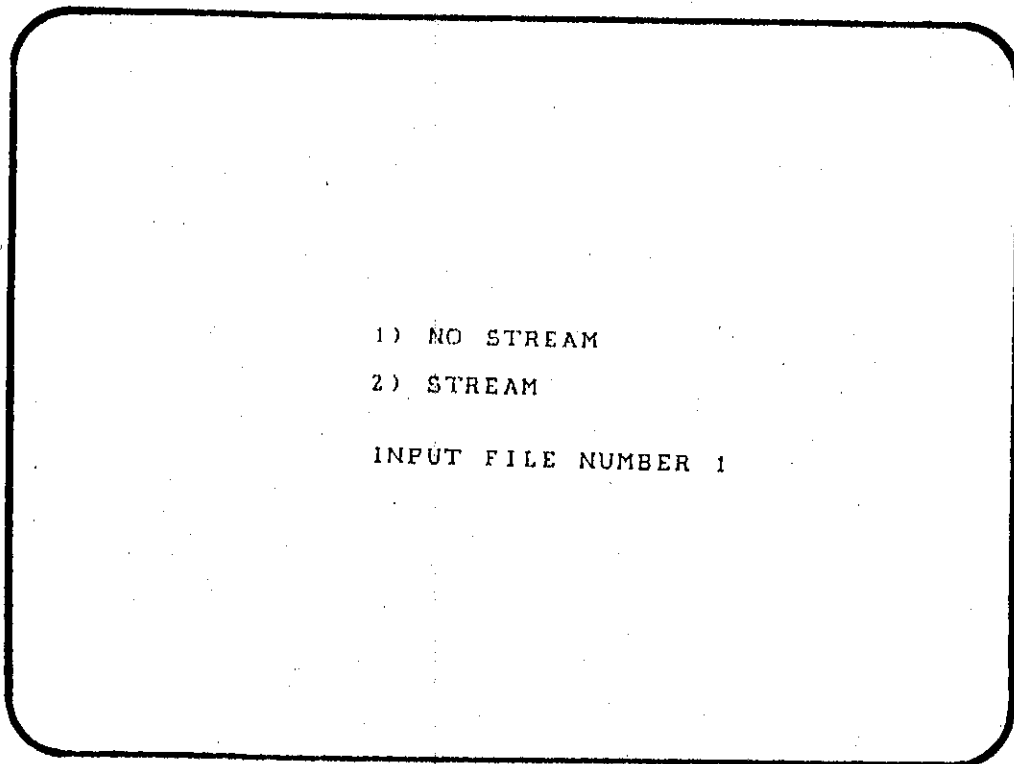


Figure B.12 - Screen Display: the files "no stream" is chosen to be plotted.

"No stream" is chosen and plotted. The "graphics display" option is again chosen with "stream" to be plotted. The program asks if the same plot is to be used (Fig. B.13).

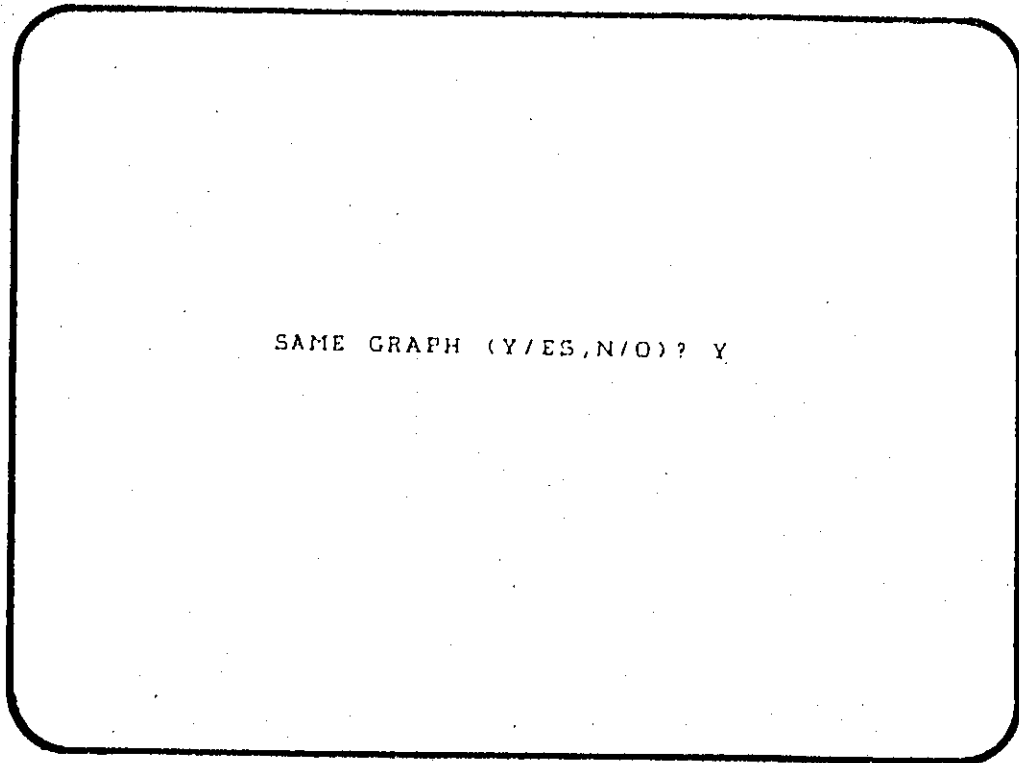


Figure B.13 - Screen Display: "stream" and "no stream" will be plotted on the same graph.

In this manner, "stream" (dotted line) and "no stream" are plotted on the same graph (Fig. B.14). With a stream in the vicinity, the mound height is lower than an infinite aquifer and not symmetric around the center basin.

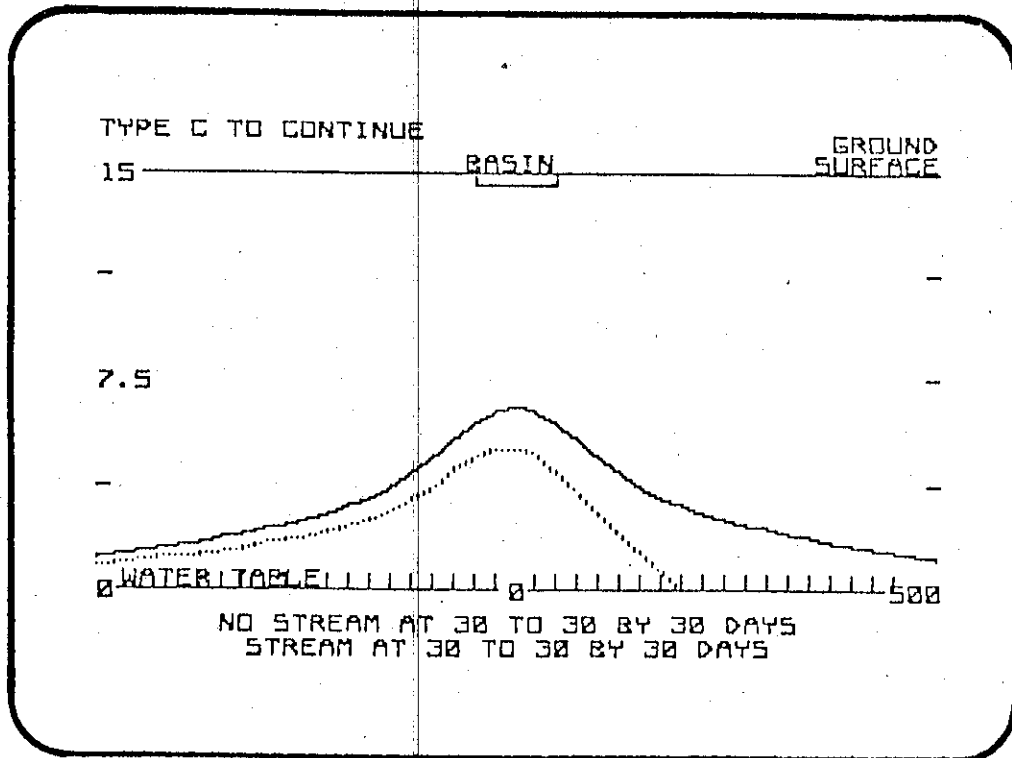


Figure B.14 - Screen Display: "stream" (dotted line) and "no stream" plotted on the same graph.

B.4 Discussion

The interactive nature of the program makes it an effective tool for a number of uses. As a learning tool, the effects of soil characteristics and constant head boundaries on artificial recharge can be studied. As a design tool, the effects of changing basin geometry or recharge rate can be examined. For those not well acquainted with groundwater, the program can be used as a demonstration tool to display the rise and decline of a water table due to artificial recharge.

Very little knowledge of computers is necessary to operate the program, yet many advantages of computer use are available. The program works by a "turn key" system, that is the disk is inserted, the computer turned on and the program begins. The user is prompted at each step, often with a variety of options. Data is easily changed, results are quickly obtained and readily compared. This ability to manipulate the problem allows for more time to be effectively spent working with the actual problem at hand.

Employment of the graphics during the operation of the program gives the user an immediate answer to the response of the aquifer. Numbers alone cannot describe the growth and decline as well as a graphical representation, especially when describing artificial recharge to a lay person. Comparison of different results is greatly enhanced by the ability to plot several different results on the same graph.

To calculate one point on the recharge mound on the APPLE computer takes about 16 seconds using APPLESOFT and 12 seconds using the compiled version of the program, compared to a small fraction of a second on the Cyber 720. For this problem, the slow speed does not cause difficulties because many points need not be calculated to give a good representation of the recharge mound. Even though execution time on a main frame computer is extremely fast, time for data input and output can be on the order of hours for one computer analysis.

For this problem memory requirements are not restrictive. The program takes about 25K bytes of random access memory leaving about 23K bytes of memory for variables. Disk utilization to store data and results greatly increases the potential storage.

The biggest limitations of the program are those which are placed on Glover's solution. Numerical models should be used if the assumptions pertaining to Glover's solution are seriously violated and data is available to describe the problem. If the field problem to be modeled is close to ideal or adequate data is not available, there is no advantage of using numerical models. This program will give results faster and cheaper.

The advent of microcomputers has given groundwater hydrologists another choice of tools for problem solving. By allowing easy communication with the problem and supplying visual results, the program demonstrates how the microcomputer can be programmed to be an effective tool. This is just one example of a large number of problems which could be solved on microcomputers.